



**TEMPLE UNIVERSITY
COLLEGE OF SCIENCE & TECHNOLOGY
DEPARTMENT OF BIOLOGY**

UNDERGRADUATE STUDENT RESEARCH SYMPOSIUM

April 29, 2024 (Monday)

9:00 AM – 5:00 PM

SERC lobby

PROGRAM

Registration: 9:00 AM

Session I: 10:00 AM – 11:30 AM

Lunch: 11:30 AM -12:30 PM

Session II: 12:30 PM -2:00 PM

SEMINAR: 2:00 PM - 3:00 PM, GLADFELTER HALL ROOM 21

From Genetic Blueprints to Biological Function:

Unraveling the Complexity of Ion Channels

Vincenzo Carnevale, Ph.D.

Bruce Taggart Associate Professor

Department of Biology, ICMS, IGEM

PRESENTATION OF DISTINCTION IN MAJOR CERTIFICATES

CST Dean Miguel Mostafá, Ph.D.

RECEPTION

Retirement of Evelyn Vleck

Assistant Professor, Department of Biology

ABSTRACTS
IN ALPHABETICAL ORDER



Understanding moss communities in temperate forest ecosystems following disturbance

Madlyn Anglin, Mary Cortese, Mariana Bonfim, Amy Freestone

Department of Biology, Temple University Ambler Field Station

Despite their abundance, only in the past few decades have mosses been recognized as important, dynamic components of northern plant communities. Mosses are integral components of forest ecosystems as they contribute to the overall biodiversity, provide crucial ecosystem functions, and can act as an indicator of a forest's health. To help understand these communities and their response to disturbance we sampled moss diversity along nine transects at three sites of varying disturbance level in a forest recently impacted by a large-scale wind disturbance. We found that diversity was variable across disturbance levels, and more closely related to habitat availability than disturbance status. This work helps us to better understand regeneration and forest recovery after disturbance events.

Effectiveness and Safety of Endoscopic Neurotomy in Managing Chronic Low Back Pain: Comprehensive Systematic Review and Meta-Analysis of 440 Cases

Yusuf Ansari, Dia Halalmeh, Saqib Hasan

Department of Biology, Temple University; Hurley Medical Center; Golden State Orthopedics and Spine

Background. Standard radiofrequency ablation techniques usually target various anatomical locations, often with limited precision regarding the exact location of the pain generator. Endoscopic ablation is a novel minimally invasive technique that increases the precision of targeting the nerve roots responsible for chronic low back pain (LBP). However, the data on long term efficacy and safety are limited.

Objective. The purpose of this study was to evaluate the safety and efficacy of endoscopic denervation for the management of chronic LBP.

Methods. A systematic search of PubMed/MEDLINE, and Cochrane Library was conducted to collect studies assessing the effectiveness and safety of endoscopic radiofrequency ablation in the treatment of chronic LBP of facetogenic or SIJ origin.

Results. A total of 12 studies with a total of 440 patients were included. The average age of patients was 63.7 ± 4.5 years with 52.8% females. Mean BMI was 25.8 ± 2.7 . All patients presented with chronic LBP, with an average duration of 55.0 ± 28.0 months. In 77.5% of cases, the source of LBP was identified as originating from the facet joints. The most common treated level was L4-5 Mean operation time was 44.0 ± 11.2 min. The preoperative VAS and ODI were 7.41 ± 0.42 and 46.1 ± 18.9 which significantly improved to 2.99 ± 1.11 and 21.9 ± 12.7 at the latest follow-up, respectively ($p < .0001$). The mean follow-up period was 17.0 ± 5.9 months. Only 2 patients (0.4%) developed complications in the form of dysesthesia. The reoperation rate was 4.09% (18/440) with a predominant majority of these cases originating from a single study (17 patients). Based on logistic regression analysis, patients with facetogenic LBP were 1.47 times more likely to have higher postoperative VAS than SIJ LBP patients ($p = .032$). There was no significant

association between age, BMI, duration of symptoms, or operation time, and postoperative outcomes (ODI or VAS).

Conclusion. The long-term clinical results of full-endoscopic denervation for chronic LBP demonstrate favorable results. Endoscopic rhizotomy is notably safe, with minimal complications. However, additional research involving a larger patient cohort and randomized controlled trials are essential to further substantiate the efficacy of endoscopic techniques as alternatives to conventional methods for chronic LBP.

Development of Edible Films that Contain α -tocopherol

Emily Arroyo, Alaina Peeler, Gregory Smutzer

Department of Biology, Temple University

Edible films are useful drug delivery systems, but these films have a limited loading capacity for most drugs. Also, these films can enhance the taste of bitter-tasting drugs or nutritional supplements. The use of long-chain fatty acids has shown promise for physically complexing drugs into microparticles that significantly increase drug loads in edible films. The goal of this project is to increase the amount of a model nutritional supplement in films while simultaneously improving the taste quality of that supplement. Vitamin E (α -tocopherol) is a nutritional supplement that is an oil at room temperature. This vitamin is orally administered in large soft gels that may represent a choking hazard for juvenile patients, elderly patients, or individuals with swallowing disorders. Our investigation revealed that complexing Vitamin E oil with stearic acid (C-18) produced a waxy compound that was then used in our film formulations. Four different film formulations were prepared and included three control formulations. These films were dried in small weigh boats. Light microscopy indicated that α -tocopherol-containing microparticles were evenly distributed in edible films. Absorption spectroscopy indicated sufficient amounts were incorporated in films. Limited studies on chemosensory perception indicated that stearic acid films exhibited a minimal taste response, α -tocopherol films exhibited a slightly oily/fatty taste response, sucralose- α -tocopherol films exhibited a strong sweet taste response, and α -tocopherol-sucralose-peppermint films offered a pleasant, sweet-cooling response. This study indicates that α -tocopherol films can be prepared that include therapeutic amounts of this nutritional supplement while enhancing the overall taste of this vitamin.

Spinal cord axon regeneration through the inhibition of novel cytoskeletal protein

Balaji Samhitha, O'Rourke Sean, Shuo Wang, Li Shuxin

Department of Biology, Temple University, Philadelphia, PA 19122; Shriners Hospitals Pediatric Research Center; Department of Anatomy and Cell Biology, Lewis Katz School of Medicine, Temple University, Philadelphia, PA 19140, USA

Introduction: Patients with central nervous system (CNS) damage face struggles in recovery due to limited axon regrowth. Spinal cord injuries lead to issues like cell apoptosis, astrogliosis, and inflammation, impairing secondary motor skills. Inhibitors around the injury site activate signals triggering cytoskeletal non-muscle myosin IIA & IIB

(NMIIA&B) protein, restricting axon elongation. NMIIA&B may bind actin filaments and form actomyosin networks to control growth cone dynamics in axons of damaged neurons. We aim to promote axon regeneration in the spine by targeting NMIIA&B.

Methods: We investigated pharmacological approaches to axon regeneration by blocking NMIIA&B in transgenic adult mice with spinal cord lesions. NMIIA&B conditional knockout mice were compared to wild-type (WT) controls after receiving adeno-associated virus type 2 (AAV2) injections and dorsal hemisections at T7 of the spine. Axon tracing and fluorescent imaging assessed axon regeneration density, while the Basso Mouse Scale (BMS) and grip strength measured motor function.

Results: We discovered significantly increased axon growth after injury in the AAV2-cre experimental group compared to WT controls. The AAV2-cre group also showed improved balance and coordination, indicating greater regeneration.

Conclusion: This study sheds light on potential molecular therapies for axon regeneration in CNS injuries, paving the way for future research to explore combination treatments with existing effective therapies.

Effects of spotted lanternfly presence on parasitic Hymenoptera community composition

Claire Becker, Mathew Helmus

Department of Biology, iEcolab, Temple University

The spotted lanternfly (SLF) has been an invasive species in the US since 2014. SLF have caused damage to several plant species because of their opportunistic feeding, and they are possibly also causing changes to compositions of insect communities such as Hymenoptera. The USDA provides the Integrative Ecology Lab (iEcoLab) with samples of Hymenoptera from sites with SLF on their preferred hosts and from sites without SLF or their preferred hosts. By identifying these insects to their family taxonomy, our lab aims to answer the question: Does presence of spotted lanternflies cause a change in the composition of parasitic and non-parasitic Hymenoptera? Research on the effects of SLF presence on local insect communities is still lacking. This identification will be accomplished using light microscopes and dichotomous keys. This will help us better understand what role SLF is taking on in local ecosystems and if it is causing community composition shifts of Hymenoptera.

When the time is right: Exploring potential niche partitioning of aquatic invertebrates in ephemeral ecosystems of a tornado-disturbed forest

Jack Brownfield, Mariana Bonfim, Mary Cortese, Amy Freestone

Department of Biology, Temple Ambler Field Station, Temple University

Unprecedented climate events are modifying landscapes and habitat structures around the globe, including the Temple Forest Observatory (TFO), which experienced large-scale destruction as a result of an EF-2 tornado in fall 2021. The habitat alteration created many ephemeral pools, which have acted as new transient ecosystems for freshwater

invertebrates. This study aims to understand the asynchronous recruitment and temporal niche partitioning of species colonizing these ephemeral pools. We compared the abundance through time, richness, and diversity of aquatic macrofauna present in the water column and surface of samples collected once a month for 12 months from 10 randomly selected ephemeral pools. We hypothesized that invertebrates will display asynchronous recruitment and therefore will fluctuate in population through time, particularly in dominant groups to better allow for coexistence between potential competitors. Analysis of collected samples has shown that major invertebrate groups do show asynchronous population recruitment, suggesting niche partitioning between potentially competitive groups. This research reveals the dynamics within these temporary ecosystems but also provides valuable insights into the broader implications of extreme climate events on habitat structure and biodiversity.

Cannabinoid modulation of opioid induced tolerance and withdrawal

Bhargav Bulusu, Sara Jane Ward

Department of Biology, Center for Substance Abuse Research, Lewis Katz School of Medicine, Philadelphia, PA.

The opioid epidemic has been an issue that has been relevant in the United States for decades, especially in the Philadelphia area. Overdosing on opioids can be lethal and accounts for thousands of deaths in our area alone. To combat opioid use disorder (OUD), my research aims to ascertain the effect of a novel synthetic cannabinoid developed by Kannalife Sciences known as KLS-13109 in opioid-induced inflammation. To achieve this, the drug was evaluated using both molecular pharmacological methods and behavioral pharmacological methods. We ran various qPCR tests which quantified the presence of the compound in various neurological receptors, completed co-immunoprecipitation procedures, and performed bicinchoninic colorimetric assays. Once these studies were used to understand the mechanism of the drug, we turned to behavioral studies to understand the drug's effects in vivo. These tests included tolerance and withdrawal studies with male mice, where KLS-13019 was used to mitigate symptoms of precipitated withdrawal.

Standing Biomass's Effect on Seed Dispersal Patterns

Brian Brown, Chris LeClair, Katherine Stevenson, Mariana Bonfim, Amy Freestone

Department of Biology, Temple Ambler Field Station, Temple University

Seed dispersal is an important mechanism used by many plants to transport their seeds away from their parent plants. In the summer of 2021, the old-growth forest, TFO was hit by an EF-2 tornado, leaving behind a severely damaged forest. To understand how our forests are adapting to anthropogenic-driven climate change it is important to understand how mechanisms, such as seed dispersal, are affected during the regeneration period of forests. To investigate how this wind disturbance has affected the forest. We collected data to compare the remaining standing biomass in TFO's focal plots to the types of dispersal found in the collected seed rain and found that standing biomass may not have

as large an influence on seed dispersal as expected. Overall, understanding the mechanisms our forests use to regenerate is important to reduce forest loss due to climate-driven disturbances. This study will help us better understand how forests respond to unnatural disturbances.

Carbonic Anhydrase Inhibitors Promote Amyloid-Beta Clearance in Alzheimer's Disease Model

Tori Brubaker, Elisa Canepa, Rafael Vazquez-Torres, Silvia Fossati

Department of Biology, Lewis Katz School of Medicine, Temple University

Alzheimer's disease (AD) is a neurodegenerative disease characterized by cognitive decline, amyloid-beta (A β) plaques, tau tangles, and severe neuroinflammation. Our lab previously investigated the effects of methazolamide (MTZ) and acetazolamide (ATZ), FDA-approved carbonic anhydrase inhibitors (CAIs), on A β pathology in TgSwDI mice (APP-Swedish-Dutch-Iowa) (1). This model is particularly suited for studying vascular A β due to the specific mutations that promote its deposition in blood vessels. We found that CAIs reduced vascular and glial A β content, and lowered neuroinflammation (1). We are now evaluating the effects of CAIs in 3xTg mice (APP, PS1, and hTau), a model that develops both A β plaques and tau tangles. We hypothesize that 3xTg mice treated with MTZ and ATZ will exhibit improved cognitive performance, reduced A β burden, and decreased neuroinflammation. Our results confirm this hypothesis, with treated mice showing improved behavioral performance, reduced A β (IHC and Thioflavin S staining), and diminished neuroinflammation.

Exploring Invertebrate Species Composition Differences to Further Analyze Metacommunity of Ephemeral Pools

Sarah N. Bucher, Mariana Bonfim, Mary R. Cortese, Amy L. Freestone

Department of Biology Temple Ambler Field Station, Temple University

In September 2021, an EF-2 tornado hit Temple University's Forest Observatory (TFO) causing substantial damage such as snapping and uprooting of trees. As the trees were uprooted, many ephemeral pools were formed, further creating new ecosystems for aquatic invertebrates to thrive in. This project aimed to explore the species composition differences among the ten ephemeral pools and the creek in TFO to further analyze if they are part of a metacommunity. To do this, samples of the creek and each pool were taken, preserved, and invertebrate species were identified using a stereoscope. Then, using PRIMER, a non-metric MDS cluster analysis was created for each season to visualize differences in composition in order to infer dispersal. By using an 80% similarity cut off, two groups of pools were identified however, further analysis of species dispersal is required to make conclusions on if they are a metacommunity.

A Novel Multidomain Potts-Hamiltonian Model to Assess Substitution Rate Heterogeneity

Sarah Chung, Lisa Schmelkin, Sudhir Kumar

Department of Biology, Temple University

As proteins evolve, the rate of substitution varies across amino acid positions. Previous studies that have modeled this variability using either a single-rate (S) or a Gamma-distributed (Γ) model consider invariant sites to best describe rates observed in protein evolution. One hypothesis is that variable rates across amino acid sites are due to coevolutionary interactions (epistasis) between multiple domains within a protein sequence. Current protein evolution models, which have used DCA approaches to infer evolution in a single domain across homologous proteins, are unable to address substitution rate heterogeneity observed in biologically relevant complex proteins. We propose a novel framework that simulates multi-domain protein evolution while considering epistatic interactions between amino acid sites. Our Joint Potts Model (JPM) simulates evolution across a tri-domain pseudo-protein, which can better model protein evolution while ensuring that all substitutions maintain structural stability. Preliminary findings reveal that while single domains may evolve at a constant rate (S), this model is not holistically applicable when evolving a whole protein sequence. Instead, we see that considering all positions of the constructed protein frequently results in Gamma-distributed (Γ) substitution rates. The development of JPM provides an advance in simulating protein evolution through an integration of complex inter-protein interactions in biologically relevant proteins.

Impact of IL-17a antibody treatment on heroin-induced IL-17a pathway signaling

Nikki Dietz, Paige Morris, Stephanie Daws

Department of Biology, Center for Substance Abuse Research, Department of Neural Sciences, Temple University, Philadelphia, PA, USA

Background: In recent years, the misuse of heroin and other opiate medications has reached epidemic levels. Opioid-induced regulation of inflammation is a consequence of opioid use. Consequentially, there has been interest in examining how various cytokines, specifically the interleukin-17 (IL-17) pathway, is affected by opioids such as heroin. IL-17a increases neutrophilic inflammation, and thus reducing IL-17a signaling may reverse heroin-induced gene expression within the brain.

Methods: We examined the effect of an IL-17a antibody on heroin-induced gene expression using a rat model. Adult male rats were treated with heroin and/or an anti-IL-17a antibody, or their controls, five times, every other day. Following the last injection, rats were euthanized, and the pre-frontal cortex (PFC) and nucleus accumbens (NAc) brain tissue were collected for molecular analysis of heroin-induced gene expression.

Results: mRNA levels of Il17ra, Il17a, Il23, Il6 and Ccl3 were measured in the PFC and NAc of rats following intermittent heroin and IL-17a antibody. There was a significant reduction of Il17ra, the receptor for IL-17a, in the animals that received heroin in combination with the IL-17a antibody, relative to the heroin group alone. Levels of Il23 in

the PFC were unchanged in all treatment groups. Levels of all transcripts of interest were unable to be detected in the NAc.

Conclusion: The IL-17a antibody may cross the blood brain barrier and is capable of impacting signaling of the IL-17a pathway. The IL-17a antibody may be a novel tool to reverse heroin-induced gene expression in the brain.

Ground Invertebrate Diversity in Varying Levels of Disturbance

Mia Engle, Mary Cortese, Mariana Bonfim, Amy Freestone

Department of Biology, Temple University Ambler Field Station

Insect diversity has been linked to forest health, with healthier forests having an increase in diversity. Additionally, insects have been shown to be highly susceptible to ecosystem disturbance events. These events reduce the likelihood of finding groups of arboreal detritivores, predacious insects, and true bugs which are all crucial for proper ecosystem functioning. In fall 2021, the Temple Ambler Field Station was hit by an EF2 tornado. We expect that ground invertebrate diversity to be directly related to the level of disturbance and subsequent change in ground cover. To understand these changes, we used pitfall traps to collect samples across sites with varying levels of disturbance during two different seasons. Data analysis has shown differences in community composition and diversity of invertebrates related to disturbance level. Some of the commonly found species in high and medium levels of disturbance include *A. hortensis*, *O. hecate*, and Lycosidae, which are part of the decomposing and predacious families. We also saw changes in community composition with season. Samples had an increase of spider species and an overall increase in abundance in the spring compared to fall. A comprehensive assessment of insects had never been completed for the Temple Ambler Field Station. This project helps to understand how the insect community may be changing due to novel disturbance events—events that are expected to increase in frequency under climate change.

The Antinociceptive and Analgesic Effects of Mitragynine and Cannabinoids in Two Mouse Pain Models

Taylor Forry, Sara Jane Ward, Mia Milton

Department of Biology, Lewis Katz School of Medicine, Center for Substance Abuse Research, Temple University

Kratom is an evergreen tree from Southeast Asia that is gaining popularity in “CBD Kratom” stores, where CBD and Kratom products are being manufactured separately and in combination products. Kratom has similar effects to CBD on individuals, such as reduced anxiety, decreased pain sensation, and increased relaxation. However, most research into the therapeutic benefits of Kratom is anecdotal. In our series of experiments, we tested how mitragynine, the most abundant active alkaloid in Kratom, affects perception of pain. In study one, we tested if mitragynine reduced pain perception. We did this via a hot plate test, where each mouse acted as its own control and then received cumulative drug dosing with hot plate trials in between each dose. We found that mitragynine did not increase the amount of time spent on the hotplate, and therefore,

likely did not affect nociception. When mitragynine was administered in conjunction with THC and CBG, it actually seemed to reduce the antinociceptive effect of these cannabinoids in higher doses. In study two, we wanted to see how mitragynine reduced inflammatory pain. We induced pain in one foot using formalin and measured the amount of time the mice spent exhibiting a pain response. We compared various doses of mitragynine to both a control group (pre-treated with saline) and a morphine group (to compare results to a typical pain reliever). We found that mitragynine at 30 mg/kg significantly reduced pain response in Phase II (late pain) of the formalin test but not Phase I (early pain).

A comprehensive comparison between evolutionary models in HyPhy and CODEML

Kathryn Gallo, Sergei Pond

Department of Biology, Institute for Genomics and Evolutionary Medicine (iGEM),
Temple University

Positive selection on advantageous genes drives evolutionary innovation; identifying whether a gene or genome is undergoing positive selection is key to understanding the genetic basis and evolutionary history of species. Several methods have been developed to identify positive selection, and codon models have become the most popular. Codon models estimate selection using the nonsynonymous to synonymous substitution rate ratio, dN/dS. Different codon models have been developed to address specific hypotheses such as testing for specific traits, codon sites, or clades of species for the presence of positive selection. In this study, we compared several codon models from the CODEML and HyPhy packages. Using various branch, site, branch-site, and clade methods, we analyzed a myxovirus (Mx) gene from ten mammals and two avian species. For the branch-site and clade models we tested specific hypotheses with different bird species. CODEML's branch-site, branch, and CMC identified each of the test branches to hold positive selection, however, BUSTED and aBSREL did not find evidence for positive selection in the chicken branch. We found that overall, CODEML's models may either be more susceptible to false positives, or have less strict requirements to detect positive selection when compared to HyPhy's models.

Control of Metabolism by Ca²⁺ in Melanoma Progression

No'ad Shanas, Scott Gross, Rohan Harollikar, Adam Karami, Alexander Armstead, MR Zaidi, J Soboloff

Department of Biology, Fels Institute for Cancer Research, Lewis Katz School of Medicine; Fox Chase Cancer Institute, Temple University

Melanoma is the fifth most diagnosed cancer in the United States. Previous research by our group found a relationship between melanoma invasiveness and suppression of store-operated calcium entry (SOCE). We also had previously found that in cells with UV-induced SOCE suppression, an increase in glucose uptake is observed without a corresponding increase in glycolysis or basal respiration. Further, RNA sequencing

showed an upregulation of enzymes associated with the hexosamine biosynthesis pathway (HBP) which favors tumor formation. Through Western blots and confocal microscopy, we found that UV radiation (or SOCE suppression through alternative means, such as genetic or pharmacological) causes a loss in mitochondrial calcium, followed by an increase in GLUT1 (glucose transport protein) expression. This excess glucose through the HBP is transformed into UDP-GlcNAc, leading to O-GlcNAcylation which we found especially prevalent in the nuclear transport proteins (NUPs). Ultimately, this contributes to higher invasion. The goal of this study is to further elucidate the parts played by mitochondrial calcium and O-GlcNAcylation in progression of melanoma.

Dopamine neuron pathway from the ventral tegmental area (VTA) to the nucleus accumbens (NAc) is non-myelinated and unaffected by short-term enhanced neuronal activity in the young mouse brain

Esther Ikpeme 1, Julia Coakley 2, Shin H. Kan g2,3

1. Department of Biology, College of Science and Technology at Temple University, 2. Department of Neural Sciences, Lewis Katz School of Medicine, 3. Shriners Hospitals Pediatric Research Center, Lewis Katz School of Medicine, Temple University, Philadelphia, PA 19140, USA

Myelin, an insulating sheath crucial for neural communication, supports efficient neural connectivity for most projection neurons. However, the myelin status of a specific set of neurons varies among different neuronal circuits, which can be regulated by age, neuronal activity, or disease. The dopamine (DA) neurons housed in the ventral tegmental area (VTA) project axons to the nucleus accumbens (NAc), forming the pivotal neural circuit for reward processing and motivational behavior. Although the VTA-NAc DA neuron connectivity is a substrate of neural plasticity, its myelin status has not been previously investigated. In this study, we used diverse genetic and chemo-genetic tools to specifically label and activate DA neurons as well as myelin-forming OLs. We found that the density of OLs is established around the VTA-NAc pathway before P15 and remains stable until at least P90. We also observed that there is no or minimal alignment between MBP+ OL processes and DA neuron axons, as well as between nodes of Ranvier-related markers and DA axons. In contrast, NF200+ projection neuron axons were highly overlapped with OL processes. Moreover, AAV-mediated chemogenetic stimulation of DA neurons did not affect the MBP+ processes near DA neurons. These results suggest that VTA-NAc DA neuron projections are poorly myelinated, and their activity does not employ new myelination as a neural plastic mechanism.

SLF-GPT: Your Comprehensive Guide to Spotted Lanternfly Research

Hannah Joseph, Matthew R. Helmus

Department of Biology, iEcolab, Temple University

Generative Pre-trained Transformers (GPT) have opened new ways in utilizing artificial intelligence as a tool in scientific research, processing a variety of information. The development of a GPT specialized for Spotted Lanternfly, *Lycorma delicatula*, research

addresses the need for comprehensive and accessible knowledge for the general community. The Spotted Lanternfly GPT, (SLF-GPT), is designed to assimilate vast amounts of data from scientific research papers and regulatory guidelines, offering insights into the biology, behavior, ecological impact, and control measures of this species. SLF-GPT enables users to understand simple to complex scientific inquiries, provide detailed information, and suggest management strategies tailored to homeowners, vineyard operators, and forestry specialists. The GPT will incorporate peer-reviewed research papers and expert guidelines, ensuring it delivers accurate, relevant, and comprehensive responses. This project aims to bridge the gap between advanced scientific research and practical, actionable knowledge for combating this invasive species. By making scientific knowledge accessible to a broader audience, it will empower communities to practice more effective management practices, contributing to mitigate the impacts of this invasive species.

Targeting Talin-Induced Integrin Activity with Natural Product Molecules: A Potential Approach in Cancer Therapy

Salvin Kabir, Jinhua Wu

Biology Department, Temple University, Fox Chase Cancer Center

This study investigates the impact of a group of natural product molecules on the specific interaction between integrin and its activator protein, talin, that mediates cellular adhesion, and derivatives of Cyanidin-3-glucoside chloride (C3G) via integrin peptide. Talin is instrumental in facilitating cell migration, invasion, and metastasis by engaging with integrin β subunits. Our investigation centers on the differential impacts of a group of natural product molecules related to Cyanidin-3-glucoside chloride (C3G), namely Cyanidin chloride (CC) and Pelargonidin chloride (PC), on the talin-integrin complex. Employing advanced protein expression and purification techniques alongside fluorescence polarization assays, we assess the binding affinities and inhibitory actions of these compounds on talin's functionality. Our findings uncover a compound-specific modulation of talin activity, where CC exhibits a marked influence on talin1 (Tln1), and PC is more effective on talin2 (Tln2). This specificity highlights the necessity of customizing therapeutic interventions to leverage distinct molecular interactions, paving the way for more targeted and efficacious cancer treatments. The insights gained from this study improve our understanding of talin's role in cellular processes and highlight its potential as a therapeutic target, advocating for a strategic approach in the development of new therapeutic agents targeting integrin-related diseases.

Women's Health and Aging Clocks: Ovarian Tissue-Specific DNA Methylation Age Predictions

Molly Kennelly, Hayan Lee

Biology Department, Temple University, Fox Chase Cancer Center

This study examines the prospects of aging in ovarian tissues through DNA methylation. Aging clocks have become notable for predicting the rate of age among various tissue

types, however, there are few studies specific to ovaries and age in the means of epigenetic clocks. Ovarian tissue methylation aging clocks are previously unexamined, and this research aims to provide insights into aging in the female reproductive system at which sites are most notable for age acceleration. Ovarian tissue samples studied were leveraged from the Genome Tissue Expression (GTEx) Project (N=164) across various ages ranging from twenties to seventies. Age groups were sectioned into decades and “Young” ages were deemed 20s - 30s and “Old” age groups included 60s - 70s. Methylation ratios were examined under these groups at different CpG sites and assessed by the topmost positive CpGs based on the difference in Old and Young methylation ratios, the topmost negative, absolute difference, and the combination of positive and negative CpGs. To determine the most valuable sites, Pearson Correlation Coefficient (PCC) calculations, Mean Absolute Error (MAE), Slope in the Aging Clock models, and Age Acceleration analysis were performed through linear regression modeling. Most recent values indicate that the topmost negative 200 CpGs have the strongest correlation of a PCC value of 0.84, an Age Acceleration value of 0.18, and a Mean Absolute Error age of less than six years (5.8). The first identified hit of a gene was identified from the CgID, cg05498649, with gene SH3BP5.

Mitogenomic: Rates of Evolution of Passerine Birds

Violet Lange 1, Maria Andreina Pacheco¹, Axl S. Cepeda, Miguel Lentino, Ananias A. Escalante¹

Department of Biology/Institute for Genomics and Evolutionary Medicine (iGEM), Temple University, Philadelphia, PA, USA 2 Colección Ornitológica Phelps, Caracas, Venezuela

Passeriformes are an order of the class Aves that includes all perching birds, which are characterized by the anisodactyl arrangement of their toes. This order makes up more than half of all extant bird species, which makes the study of passerine phylogenetics very important. Evolutionary biologists are heavily studying the phylogeny of this order due to its high morphological diversity and massive evolutionary radiation. Here, five new complete passerine mitochondrial genome (mtDNA) sequences are reported and aligned with 383 other passerine mtDNA sequences available in the GenBank using MAFFT software. Then, a maximum likelihood method was applied to estimate the phylogenetic tree using IQ-Tree software, and mtDNA sequences of closely related orders, including Falconiformes and Psittaciformes, were used as outgroups. Results were compared with previously published phylogenies using whole nuclear genomes. It was found that the phylogeny using mitochondrial genomes is consistent with previously reported phylogenies, with few discrepancies due to a lack of genome availability (sampling) or modifications to taxonomy. RelTime, a software that estimates evolutionary rates of species at every branching point on the tree, was implemented to approximate the rate of divergence of passerines. The evolutionary rates of the order Passeriformes will be discussed, and in the future, this phylogeny will be used to analyze the divergence times of passerine families.

Investigating Constraints on the Evolution of Floral Longevity in *Sabatia angularis*

Amanda Le, Rachel Spigler

Department of Biology, Temple University

Floral longevity is a critical determinant of reproductive success in plants, yet empirical research on its evolution within species is notably lacking. Evolutionary frameworks for understanding floral longevity are rooted in resource allocation theory, putting forth the concept that selection acts upon heritable variation to optimize floral longevity considering competing construction and maintenance costs. However, critical assumptions of these models remain untested within natural populations. We collected data on floral longevity and other key reproductive traits from individuals in an artificial selection study. Specifically, we measured petal area and flower mass, and counted flower number and ovule number per flower. By examining the impact of artificial selection for floral longevity within artificially selected populations, we were able to gain a better understand of genetic correlations involving floral longevity dynamics, the mechanisms shaping plant reproduction. More broadly it provides insights on resource allocation, fitness, and evolutionary strategies in natural populations.

The Impact of Cigarette Smoke and Ethanol Co-exposure on Mice

Esmeralda Lua 1,2, Zoe M. Davis-Luizer 1,2, Hassan Haya k1,2, Karim Bahmed 1,2,3, Ellen Unterwald 4,5, T. K. Eisenstein 4,5, Beata Kosmider 1,2,3

Department of Biology, 1. Department of Microbiology, Immunology, and Inflammation, 2. Center for Inflammation and Lung Research, 3. Department of Thoracic Medicine and Surgery, 4. Department of Neural Sciences, 5. Center for Substance Abuse Research, Temple University, Philadelphia, PA 19140, USA

The most prevalent forms of substance abuse involve tobacco, in the form of cigarette smoking, and alcohol consumption, in the form of ethanol. However, the impact of the co-exposure in relation to lung injury is not widely understood or researched. The trajectory of the experiments outlined herein aims toward understanding the impacts of this co-abuse through examining gender differences of mice exposed to cigarette, ethanol, and co-exposed to cigarette smoke and ethanol. Smoking was administered for 2 hours at the same time every day, 5 days a week for 4 weeks. Following exposure to cigarette smoke, 10% ethanol was provided in the enclosure for approximately 21 hours. A statistically significant difference was observed in males, revealing heightened DNA levels in the plasma following exposure to cigarette smoke (CS) and ethanol. In contrast, females exhibited elevated GPC6 and GRM7 gene expression in response to cigarette smoke and ethanol exposure. Analysis of male and female mice also showed a decrease in mitochondrial DNA after cigarette smoke and ethanol exposure. Notably, a pronounced decline in female mice was detected, suggesting an impact on mitochondrial function in this group. Furthermore, protein expression was analyzed by Western blotting to define a pro-inflammatory response in murine lung tissue. Understanding the combined effects of cigarette smoke and alcohol consumption on lung injury is important to advance our knowledge of lung disease pathophysiology. It also aids in fostering the development of

innovative therapeutics targeting respiratory dysfunction.

Liposomes Interactions with Platelets via Fluorescence Spectroscopy

Imene Mancer, Michelle Tanujaya, Parkson Lee-Gau Chong

Department of Biology, Department of Molecular Biochemistry and Medical Genetics,
Lewis Katz School of Medicine, Temple University, Philadelphia, PA, USA

DPA-Cy3[22,22] and POPC liposomes as resilient vehicles for targeted drug delivery and antithrombotic applications. Tailored mole ratios and analyses, including fluorescence quenching, underscore their stability and selective binding, especially with MCF-7 breast cancer cells. Fluorescence energy transfer is utilized to study the interactions of DPAL: antithrombotic liposomes with platelets. Laurdan, a fluorescent membrane probe labeling platelets, as the energy transfer donor. Cy3, a fluorophore embedded in the liposomes, as an energy transfer. The emission spectrum of Laurdan was observed in the presence of varying amounts of DPAL liposomes. An increase in Cy3 fluorescence was observed at 575 nm and a decrease in Laurdan fluorescence at 430 as a DPAL is added to platelets, indicative of energy transfer due to binding of DPAL to platelets. Findings affirm the enduring stability of these liposomes, as well, ultimately positions them as pivotal in advancing targeted drug delivery and antithrombotic interventions.

WEE1 inhibition Synergistic targets

Logan McCullough, Theodore Nguyen, Erica Golemis

Department of Biology, Temple University, Fox Chase Cancer Center

Globally, HNSCC enlists more than 800,000 new cases and 165,000 deaths annually. HNSCC is generally divided into two subsets, these being HPV+ (Human papillomavirus) and HPV-. HPV plays a critical role in upregulating the risk for development of HNSCC as HPV protrudes various complications in the essential maintenance and regulation of cellular machinery. Furthermore, HPV- HNSCC most frequently associated risk factor is the use of tobacco and alcohol, alone and in combination. HPV- HNSCC is more frequent and often associated with inimical consequences. The patriarch of risk factors presents TP53 and CDKN2A tumor suppressors and check point mediator mutations as common precursors to the development of HNSCC. Consequently, reliance upon alternative checkpoint regulators such as, WEE1 kinase becomes increasingly pronounced in efforts to attenuate DNA damage and replication stress. WEE1 inhibition typically administered through adavosertib is a throughput method of treatment currently in clinical trials. Our previous data shows WEE1 inhibition delegates glycolytic intermediates to alter course into the Pentose Phosphate Pathway (PPP) as a mediation of nucleotide depletion due to replication stress. Through the proceeding experiments we aim to identify potential synergistic targets for WEE1 inhibition at various stages of the transition from glycolysis to the PPP. Thus far, methotrexate, NCT-503, and COH-29 show synergistic effects, observing reduced cell viability in clonogenic survival assays, and cell cycle progression inhibition.

Salmonid Myostatin Pathway Diversification as a Result of Whole Gene Duplication Events

Laura McDonnell, Amanda E. Wilson, David A. Liberles

Department of Biology and Center for Computational Genetics and Genomics, Temple University

Whole genome duplication (WGD) events have significant implications for organismal evolution, particularly in shaping pathway structures and the specificity of interactions among proteins. WGD is a mechanism that can create entire new pathways in parallel from existing single pathways. Our study aims to elucidate this process, focusing on myostatin (TGF-beta signaling) in salmonids as a model system. We leverage data from various databases, alongside amino acid and nucleotide sequences of salmonids (2WGD events) together with zebrafish (1 WGD event) and mice (0 WGD events), to construct gene trees involving myostatin and two of its interacting partners: activin type II receptors and follistatin. This approach provides insights into gene loss and divergence among duplicate gene copies for sets of interacting proteins. Furthermore, structural modeling and docking programs are employed to assess changes in protein structure and their potential impact on binding interactions. The overarching goal is to understand how WGD events influence pathway evolution. Currently, reconciled gene trees have been generated for this set of three species. Ongoing steps involve conducting structural modeling including docking to determine structural divergence of gene products and the resulting effect on binding activity. By dissecting the dynamics of myostatin and its interacting partners in salmonids, zebrafish, and mice, we not only contribute to fundamental knowledge about pathway evolution but also unveil novel insights into myostatin signaling.

Invasive Pioneer Plant Species Presence in Differently Disturbed Temperate Old-Growth Forests

Kelly Meinert, Christopher LeClair, Mariana Bonfim, Mary R. Cortese, Amy L. Freestone, Brent J. Sewall

Department of Biology, College of Science and Technology, Temple Ambler Field Station, Temple University

On September 1st, 2021, Temple University's Ambler Campus was unexpectedly hit by a tornado with highly destructive 130 mph wind speeds, brought upon by the remnants of Hurricane Ida. This large-scale wind disturbance provided a unique opportunity to study invasion by numerous previously absent non-native herbaceous and woody understory pioneer plant species into areas of two old-growth forests that experienced different impacts of the tornado. As a result, the goal of this project was to determine whether the composition, abundance, richness, and distribution of these invasive pioneer plants had a relationship to relative disturbance levels at the two old-growth forest sites assessed. For this evaluation, a visual percent cover survey of 13 focal invasive understory pioneer plant species was performed in the summer of 2023, and relative disturbance values were calculated as a function of the percent forest canopy cover over the areas surveyed. Results hint at overall invasive species abundance and richness being higher at the

disturbed forest site (Temple Forest Observatory, TFO) than at the undisturbed forest site (Robbins Park Environmental Education Center, RBP). These findings are significant because the competitive interactions between native and non-native species currently being observed within the understory layer of this recovering forest system may provide insight into the factors underlying the success of regeneration of dominant overstory tree species in recently heavily disturbed forests.

The Effects of Proximal vs. Distal Synaptic Transmission of Signals in Neural Circuitry

Gabriella Mercado, Brandon Hugger, James Rosado, Gillian Queisser, Benjamin Seibold

Department of Biology, Department of Mathematics, College of Science and Technology, Temple University, Philadelphia PA,

Understanding synaptic transmission within neural networks is crucial for unveiling the complex dynamics of brain function. In this study, the use of an innovative approach using virtual reality (VR) simulation to investigate synaptic transmission across neural circuits. By manipulating VR technology and creating realistic three-dimensional models of neural networks, the interactive exploration of synaptic connectivity and dynamics was conducted. This study focused on analyzing the patterns of special proximity in synaptic transmission and its impact on the functionalization of signal processing. Through a series of experiments, the dynamics of synaptic connections and signal transmission was characterized including network-level synchronization. The NeuroVISOR technology is a software employed with advanced computation algorithms that allow for analysis of data generated from VR simulations. These data provide insight into mechanisms of underlying synaptic integration and informational processing within neural circuits. Findings of this study are able to contribute to the growing knowledge of synaptic function and neural network kinetics while also demonstrating the potential of VR simulation being used in further research as a tool for investigating these complex processes. This study allows for open avenues for understanding brain function and developing revolutionary interventions for neurological disorders.

ZNF362 (Lin-29) as a Potential Therapeutic Target for Spinal Cord Injury Repair and Recovery

Ganesh Muruganandam, Ha Neui Kim, Shuxin Li

Department of Biology, Shriners Hospitals Pediatric Research Center, Department of Neural Sciences, Lewis Katz School of Medicine at Temple University, Philadelphia, PA 19140, USA

Spinal cord injuries (SCIs) can cause paralysis by severing the axons in the corticospinal tract (CST). These injuries are often permanent as mature neurons in the mammalian central nervous system (CNS), theoretically, cannot regrow their axons despite having had the capability to do so before maturation. Many studies have examined the genes regulating the intrinsic growth capacity of these neurons, but various other unidentified

pathways exist that could also be targeted to promote axon regeneration. ZNF362 (Alias: Lin-29) is a gene encoding a zinc finger transcription factor that participates in a heterochronic pathway involved in the juvenile-adult transition in many tissues, including the neuronal tissue, of *Caenorhabditis elegans* and possibly mammals. In this project, we examined whether inhibiting Lin-29 in CST neurons would stimulate post-SCI axon regrowth using mouse models. We compared the extent of axon regeneration and the course of functional recovery between adult Lin-29 conditional knockout (cKO) mice and wild-type (WT) mice with procedurally generated SCIs. Notably, knocking out Lin-29 expression in select CST neurons resulted in fairly better axonal regeneration in the descending spinal tracts below the SCI lesion. Locomotor recovery was also shown to be better in Lin-29 cKO mice compared to WT mice. These results indicate that ZNF362 (Lin-29) may play a critical role in modulating axon regeneration in mature CST neurons and could serve as an effective molecular target for SCI treatments.

Preliminary Pharmaceutical Properties of CBD Oral Films

Olivia Oxenreider, Gregory Smutzer

Department of Biology, Temple University

This study exploited microparticle preparations that physically complex solid CBD with long-chain fatty alcohols (stearyl alcohol) or long-chain fatty acids (stearic acid) by the hot-melt method. Next, the physical properties of these films were examined in detail. These properties include quantification of CBD in microparticles, in vitro dissolution assays, and size measurements and distribution of microparticles in films. This set of experiment worked towards determining the standard concentration of the CBD used in the oral films, optimizing dissolution study methods to yield replicable results, and determine the average size and distribution of CBD microparticles in the films. Through the evaluation of several methods for dissolution assays, the most optimized procedure was found to include sampling of the solution via centrifuge tubes and combining the samples with acetonitrile. The average microparticle area was found to be 0.0247 mm² with an average perimeter of 0.6197 mm. A calibration curve of the CBD used in the films was generated with an R² of 0.9878.

From Theory to Practice: Hands-on Exploration of Environmental Resilience at Ambler Field Station

Ji Pan, Mariana Bonfim

Department of Biology, Temple Ambler Field Station, Temple University

Teaching about ecological concepts such as species richness and the Intermediate Disturbance Hypothesis (IDH) presents unique challenges due to the dynamic nature of ecosystems and environmental gradients. According to IDH, ecosystems experiencing moderate disturbance levels foster greater biodiversity by creating opportunities for new species while maintaining the presence of resilient species. This concept is further enhanced by edge effects, which define habitats as discrete patches where boundaries between them and the surrounding matrix experience heightened levels of disturbance.

Navigating these concepts requires students to understand nuanced interactions between ecological processes and environmental gradients, and the Temple Ambler Field Station serves as an invaluable resource for fostering hands-on opportunities to explore critical thinking and problem-solving skills essential for addressing contemporary environmental issues. Using transect-quadrat sampling we examined if plant species richness was highest at sites that experienced intermediate levels of disturbance by a recent tornado disturbance. Further, we administered a brief survey to students who participated in this field data collection to gauge the effectiveness of these activities on their learning outcomes. Student participation in investigating the impact of large-scale disturbances, such as the EF-2 tornado, provides valuable insights into the effects of climate-related events on ecosystems. By engaging with Field Station's activities, students gain a deeper appreciation for the environment and are better prepared to contribute to multidisciplinary solutions for mitigating the impacts of climate change in the future.

Efficacy of Ketamine to Regulate eEF2 in Female Mice

Leon Passarelli-Roberts, Xiangdang Shi, Mary McCafferty, Ellen Unterwald

Department of Biology, Center for Substance Abuse Research, Department of Neural Sciences, Lewis Katz School of Medicine, Temple University

Ketamine is a novel therapeutic with antidepressant qualities that can aid people with treatment-resistant major depressive disorder. One of ketamine's mechanisms of action occurs through its blockade of post-synaptic NMDA receptors. By blocking NMDARs, calcium influx into the neuron is reduced. In turn, this causes a phosphorylation cascade that then leads to the phosphorylation and inactivation of the protein eEF2. eEF2's is significant, as it is an elongation factor involved in protein synthesis. My project sought to find at what time-point an acute administration of ketamine causes a decrease of phosphorylated eEF2 levels in female mice. I hypothesized that ketamine would regulate eEF2 activity via phosphorylation after 60 minutes. To study this, 8-week-old female C57BL6 mice were given a single injection of either ketamine (10 mg/kg) or saline. The animals were sacrificed after wither 30 or 60 minutes. After this, the PFC of the mice were collected. Protein levels were determined using Western blotting. Proteins of interest were phospho-eEF2 (Threonine 56) and eEF2. Current results suggest that 30- and 60-minutes post-administration of ketamine show no significant change in phosphorylation levels. This conclusion reflects results found investigating the protein GSK3 β , which further shows the importance of clear methods reported on research papers, as results often found in male mice do not always translate to female subjects. Future directions for this project include using smaller doses of ketamine for the mice, as some research suggest a better response. As well, to use male mice to compare potential sex differences in protein activity.

Sex differences in a mouse model of melanoma

Kiera Patton, Dan Deegan, Raza N, Gillian McGuire, Nora Engel

Department of Biology, Temple University, Coriell Institute

Melanoma exhibits significant differences in mortality between males and females in epidemiologic data. Males have a mortality rate of 4.09 and females have a mortality rate of 1.7 according to a recent metaanalysis. This may be partially explained by behavior but even controlling for that the difference remains. The exact reason for this disparity is unclear, though some immunological differences have been identified. Males also tend to have more melanomas in the head and neck region while females have more melanomas in the extremities. In this paper we examine the role of sex and age in melanoma through analysis of the TCGA cancer database in R in hopes of finding out more about the biochemical and genetic basis of this sex difference in melanoma. We examine the transcriptional landscape of melanoma with respect to age and sex through analysis of TCGA RNAseq data.

Investigating the Impact of 5-methylcytosine (5mC) and 5-hydroxymethylcytosine (5 hmC) on Alzheimer's Disease Pathogenesis

Dominyka Petraskaite, Hayan Lee

Department of Biology, Temple University, Fox Chase Cancer Institute

Alzheimer's disease (AD) stands as a significant cause of both mortality and dementia, with existing treatments mainly focused on symptom management rather than altering the disease's trajectory. This study delves into the epigenetic intricacies of AD by exploring the roles of 5-hydroxymethylcytosine (5hmC) and 5-methylcytosine (5mC), which have shown promise as biomarkers for shedding light on AD's pathology. Leveraging advanced statistical and visualization techniques in Python to conduct a secondary analysis of the GSE109627 dataset (tissue: middle temporal gyrus), we identified unique methylation patterns in AD compared to control brain tissues. Our findings highlight marked epigenetic disparities that align with AD's progression, suggesting these modifications play a key role in the disease's underlying mechanisms. While acknowledging the study's limitations, such as sample diversity and conversion methodologies, we underline the significance of methylation and hydroxymethylation in understanding AD. This research points to an encouraging path for future therapeutic interventions. It emphasizes the necessity for further investigations with more diverse and extensive datasets to solidify the role of epigenetic modifications as AD biomarkers. In doing so, it lays a groundwork for subsequent studies aimed at deciphering AD's complexities, contributing significantly to the field of precision medicine in managing neurodegenerative diseases.

Chemogenetic Manipulation of Indirect Pathway in Parkinson's Disease via Subthalamic Nucleus Compares Favorably to AAV-GAD Therapy

Sraavya Pinjala, Nassim Stegamat, George Smith

Department of Biology, Shriners Hospitals Pediatric Research Center, Department of Neural Sciences, Lewis Katz School of Medicine, Temple University, Philadelphia, PA 19140, USA

Parkinson's disease (PD) is a neurodegenerative disorder in which the dopaminergic neurons in the substantia nigra degenerate, thus resulting in abnormal activity in the basal ganglia. The primary function of the basal ganglion is to initiate and terminate movements, which is disrupted in PD. The loss of dopaminergic neurons in the substantia nigra causes increased activation of the movement termination pathway through the subthalamic nucleus (STN), in the basal ganglia. This is reflected in symptoms of Parkinson's disease including dyskinesia, muscle rigidity, and postural instability. In 2002, Dr. Luo and Colleagues conducted an experiment in which Glutamic Acid Decarboxylase (GAD) was overexpressed in the Subthalamic Nucleus to upregulate GABA production, with the idea that the inhibitory effect of GABA would mitigate the hyperexcited activity of the subthalamic nucleus, thereby reducing rigidity and improving movement. While the Luo paper relies on the inactivation of the overexcited STN, we hypothesized that in the rat 6-hydroxydopamine Parkinson's model could benefit from treatment with excitatory DREADDs to drive inhibition of the target of the subthalamic nucleus. Lesioned rats were injected with Excitatory DREADDs (Designer Receptor Exclusively Activated by Designer Drugs) to drive the release of GABA from the GAD65 synapses. DREADDs and GAD are co-transduced neurons, so most neurons express both. Therefore, the activation of the excitatory DREADDs by Clozapine n-oxide (CNO) induces the release of GABA, from the glutaminergic terminals (excitatory) to reverse excitation to promote inhibition. In normal Parkinson's the STN becomes excitatory which causes dyskinesia, therefore this inhibitory reaction should then decrease the physiological impacts of the Parkinson's inducing lesion while exciting the necessary pathways. The results of the study were analyzed behaviorally via a decrease in ipsi-lesional rotation rates and symmetry in limb preference. Decreased ipsi-lesional rotations and limb symmetry were observed in rats treated with excitatory DREADDs 5 weeks post-lesion.

Restoring pVHL interactions in mutant clear cell renal cell carcinoma with a small molecule

Sarah Sahotra, John Karanicolos

Department of Biology, Temple University, Fox Chase Cancer Institute

Kidney cancer, particularly clear cell renal cell carcinoma (ccRCC), ranked among the top ten most reported cancers worldwide, with a notable prominence in the North American region. The von Hippel-Lindau (VHL) protein, a crucial tumor suppressor located on chromosome 3 is commonly mutated in ccRCC. It operates as the substrate recognition element within the VHL E3 ubiquitin ligase complex, it targets hypoxia-inducible factor (HIF) for degradation under normoxic conditions, restraining the activation of genes

associated with angiogenesis, glycolysis, and cell survival. Dysregulation of VHL is notably linked to clear cell renal cell carcinoma (ccRCC), characterized by highly vascularized kidney tumors. CP4.29 is a newly designed molecule in Karanicolas Lab, FCCC, that acts as a mutant VHL refolder. To unravel the complex interplay of VHL with various substrates, a dual-method approach was employed. The AirlID experiment detected pVHL interactions in renal cancer cells, followed by AlphaFold modeling to understand the protein structures. Proximity-dependent biotinylation using BioID allowed the identification of protein-protein interactions within live cells, and mass spectrometry provided detailed profiling of the VHL interactome. Leveraging AlphaFold2, structural models of 109 up-regulated and 123 down-regulated proteins were generated and stratified based on machine learning interaction scores to find that the interactor substrates were docked into the alpha helix and beta sheet of VHL. Clustering the interactor proteins within certain functional pathways, we found enrichment of the endoplasmic reticulum associated ribosomes, chaperones, and membrane components. Then we validated these CP4.29 induced VHL interactions by silencing and confirming the loss of CP4.29 activity with the loss of elongin C and SRP9. This integrated analysis enhances our understanding of pVHL interactions in renal cancer and offers potential targets for focused therapeutic strategies.

Characterization of novel effectors in the progranulin/EphA2 axis in bladder cancer

Vruna Satasiya, Sharon Burk, Antonio Giordano, Andrea Morrione

Sbarro Institute for Cancer Research and Molecular Medicine, Center for Biotechnology, Department of Biology, College of Science and Technology, Temple University

Bladder cancer is one of the most common malignancies, and it represents the ninth most common cancer diagnosis in the world. It is associated with substantial morbidity and mortality due to the burden of treatment and the cost of care for this malignancy. Progranulin is a pluripotent growth factor whose dysregulation is implicated in several human pathologies including frontotemporal dementia, inflammation, immune response and cancer. Its pro-tumorigenic action is linked to the activation of its receptor, EphA2, a member of a large family of receptor tyrosine kinases. In bladder cancer, we previously discovered that progranulin stimulates EphA2 phosphorylation at Ser897, which leads to enhanced tumor cell motility, invasion, and in vivo growth. We also demonstrated that EphA2 depletion significantly diminished progranulin-dependent motility and anchorage-independent growth, while enhancing sensitivity of bladder cancer cells to cisplatin treatment. In recent years, the progranulin/EphA2 axis has emerged as a critical pathway in bladder cancer progression, but the molecular details of action are still poorly defined. We recently conducted mass spectrometry analysis and identified novel progranulin-dependent EphA2 interactors including FAM120A, which is a protein with a putative role in oncogenic pathways. We discovered that FAM120A is significantly expressed in urothelial carcinoma cells. Importantly, we also demonstrate the EphA2 complex with FAM120A in progranulin-dependent manner. Moreover, using immunofluorescence analysis we showed that EphA2 and FAM120A colocalized upon progranulin stimulation.

Overall, this research offers insights into the progranulin/EphA2 signaling axis and uncover new effectors for a better understanding of bladder cancer progression.

Bmi1 Mediates Repair Post-Myocardial Injury by Modulation of Fibrosis

Faiz H Siddiqui, Lindsay Kraus PhD, Tabito Kino, and Sadia Mohsin

Department of Biology, Aging + Cardiovascular Discovery Center, Lewis Katz School of Medicine, Temple University, Philadelphia, PA 19140

Cardiovascular Disease (CVD) is a devastating and increasing concern across the globe leading to myocardial injury. Worldwide, CVDs are the leading cause of death, with about 18 million deaths annually. Myocardial injury can lead to decay, overall cardiac dysfunction, and buildup of scar tissue through sustained cardiac fibrosis. Fibroblasts in the heart produce the extracellular matrix which contributes to the stiffening of tissue post-injury in their role as the main cell type to promote cardiac fibrosis. The transforming growth factor (TGFB) is a protein that induces the activation of these isolated fibroblasts, which can be used to visualize fibrosis in the heart. The Polycomb complex protein BMI-1 (Bmi1), an epigenetic regulator, is associated with numerous biological functions including mediating DNA damage and apoptosis. Currently, there is a lack of understanding of how Bmi1 mediates epigenetic modifications influencing cardiac fibroblasts and fibrosis in the cardiac areas.

Effect of Disturbance on the Composition of Mushroom Colonies Through Time

Lana Stoy, Mary Cortese, Mariana Bonfim

Biology Department and Ambler Field Station

In September 2021, an EF2 tornado struck the Temple Forest Observatory (TFO) dramatically altering forest structure. With altered forest structure we also expected changes to closely coexisting fungal communities. We wanted to understand how the abundance and richness of mushroom colonies has changed in the three years of forest succession following the storm. We expect fungal abundance to increase due to the increase in decaying biomass and fungal richness to decrease due to competitive dominance. We retrieved data from six quadrants across TFO and Robbins Park, our control site. We then compared data to survey data from 2022 and 2023. Our results showed differences in community composition at different years as well as varying abundance between our disturbed and undisturbed site. This research helps us to better understand mushrooms role as an indicator for an ecosystem's health and forest recovery.

Effects of Troriluzole on Anxiety- and Depression-like Behaviors in Methamphetamine-Naive and Methamphetamine-Abstinent Mice

Ola Szmecinski 1, Sonita Wiah 2, Samhitha Reddy 3, Megha Varghese 1, Jordyn Chambers 1, Scott Rawls 2

1. Department of Biology, College of Science and Technology; 2. Center for Substance Abuse Research, Lewis Katz School of Medicine; 3. Psychology Department, College of Liberal Arts, Temple University, Philadelphia, PA

Troriluzole (TRLZ) is a prodrug of riluzole (RLZ), an FDA-approved drug for amyotrophic lateral sclerosis (ALS), that reduces glutamate neurotransmission by reducing glutamate release and enhancing glutamate reuptake. TRLZ, in bypassing pharmacokinetic limitations experienced with RLZ, has the potential to normalize the glutamate dysregulation seen in anxiety and depression alone and as symptoms of methamphetamine (METH) withdrawal. Anxiety-like behavior of mice was measured with the elevated plus maze (EPM), while depression-like behavior was assayed with the forced swim test (FST). Behavioral sensitization to METH was measured with the locomotor test. Acute TRLZ administration at 3 doses (4 mg/kg, 8 mg/kg, 12 mg/kg) resulted in an anxiolytic effect at higher doses (8 mg/kg, 12 mg/kg) but no anti-depressive effect at any doses. A 10-day METH and TRLZ binge was performed in order to establish METH dependence. Chronic TRLZ administration alongside METH exposure resulted in an anti-depressive effect, but no anxiolytic effect, during METH abstinence. TRLZ also reduced locomotor sensitization to METH following the binge, indicating reduced drug cravings in the mice. The seemingly contradictory effects of acute and chronic TRLZ indicate potential differences in TRLZ's effects on behavior with time and in the context of METH. The anxiolytic effects of acute TRLZ suggest that TRLZ can be indicated for rapid anxiety relief. The anti-depressive effects and reduced behavioral sensitization of chronic TRLZ with chronic METH exposure suggest that TRLZ has the potential to reduce METH withdrawal symptoms and drug cravings, thus reducing the risk of relapse.

Investigating Y155 Phosphorylation of Protein Kinase C δ on Blood Platelets as a Model for Neuronal Disease Mechanisms

Dhruv N Vajipayajula, Carol Dangelmaier, Monica Wright, Satya P Kunapuli

Department of Biology and Sol Sherry Thrombosis Research Center, Lewis Katz School of Medicine, Temple University

Neurons and platelets, although vastly different in origin and function, exhibit several similarities in their molecular composition and signaling mechanisms. This paper attempts to evaluate platelets as "circulating mirrors of neurons", with a particular focus on Protein Kinase C – Delta (PKC δ). PKC δ is involved in many neuronal disease states including inflammation and degeneration. We demonstrate that PKC δ phosphorylation at the Y155 residue occurs specifically in response to the activation of the Glycoprotein receptor VI pathway (GPVI), physiologically stimulated by collagen. Using PKC δ Y155 knock-in mice, we show its involvement in GPVI mediated platelet activation and thrombus formation both ex-vivo and in-vivo. Our findings suggest a specific role for Y155 phosphorylation in PKC δ -associated signaling. We underscore the potential of platelets as accessible

models for neuronal signaling pathways and we propose implications of PKC δ Y155 phosphorylation in probing neurodegenerative and inflammatory disease processes.

Establishing the Effects of Alcohol on Human Induced Pluripotent Stem Cells (hiPSCs) and hiPSC-derived Human Cerebral Organoids (hCOs)

Madison Wolf, Martina Donadoni, Senem Çakir, Ilker K. Sariyer

Department of Biology, Department of Microbiology, Immunology and Inflammation,
Center for Neurovirology & Gene Editing, Temple University Lewis Katz School of
Medicine, Philadelphia, PA 19140 USA

Alcohol use disorders (AUDs) are the most common pathologies affecting the central nervous system (CNS). Fetal alcohol exposure is known to impact brain development and have cognitive and behavioral deficits collectively referred to as Fetal Alcohol Spectrum Disorders (FASDs). Myeloid cell leukemia 1 (Mcl-1) protein is a pro-survival member of the Bcl-2 family. Mcl-1 has two major isoforms, Mcl-1L and Mcl-1S. Several studies have shown that the Mcl-1L isoform enhances cell survival by inhibiting apoptosis, while Mcl-1S promotes apoptosis. Previous studies by our lab have demonstrated that missplicing of Mcl-1 and the favoring of Mcl-1S splicing over the Mcl-1L gene product has been associated with ethanol-induced toxicity within the context of the CNS. Here, we investigated the effect of alcohol insult on Mcl-1 pre-mRNA splicing in human induced pluripotent stem cells (hiPSCs) and human cerebral organoids (hCO) models. We assessed cell viability following ethanol treatment using MTT analysis and analyzed mRNA expression of Mcl-1 isoforms via RT-PCR and ddPCR. Furthermore, we analyzed protein expression of isoforms via Western blotting. Our results suggest that protein expression of the Mcl-1L isoform decreases in hiPSCs following ethanol exposure in a dose-dependent manner. Additionally, acute alcohol treatment induces alternative splicing of the Mcl-1S isoform in hiPSCs and hCOs in a dose-dependent manner. Our results provide empirical evidence that dysregulation of Mcl-1 alternative pre-mRNA splicing by alcohol in progenitor cells may play a key role in development of fetal alcohol syndrome and be a novel target of developing therapeutic interventions.

Epigenetic changes in development of Myelomeningocele

Kuralai Zholdosh kyzy, Karolina Janik, Barbara Krynska

Department of Biology, Lewis Katz School of Medicine, Shriners Hospitals Pediatric
Research Center, Temple University

Myelomeningocele (MMC) is a severe congenital defect characterized by the failure of neural tube closure, which affects the development and function of the spinal cord. Astrocytosis constitutes one of the pathological features of the developing MMC spinal cord, but the mechanism underlying this abnormal development of astrocytes remains poorly understood. Epigenetic changes, such as histone modifications, are an important component of the machinery involved in the fundamental process of astrocytes development. Using a retinoic acid-induced fetal rat model of MMC, we investigated methylation levels of histone 3 lysine 4 (H3K4), which is a permissive histone mark during

differentiation of neural progenitors into astrocytes, and compared patterns of H3K4 methylation in different regions of MMC spinal cords with those in normal controls in the context of astrocyte development. Our findings revealed significantly higher levels of methylated H3K4 (H3K4me) in developing MMC spinal cords compared to age-matched controls during ongoing astrogenesis. The methylated H3K4 strongly co-localized with markers of astrocyte progenitors in MMC spinal cord. This was paralleled by increased expression of aldehyde dehydrogenase type 1L1 (ALDH1L1) and glial fibrillary acidic protein (GFAP), markers of differentiating astrocytes, resulting in accelerated timing and magnitude of astrocytes generation in MMC spinal cords. Our results demonstrated modifications of H3K4 methylation, which is a permissive epigenetic factor involved in initiation of neural progenitors differentiation into astrocytes during normal astrocytes development. These novel findings suggest that epigenetic changes, such as histone methylation, may be involved in the process of abnormal development of astrocytes in MMC spinal cord.

POSTER NUMBERS

- P1. Ikpeme, E.,** Cellular & Molecular Neuroscience
Dopamine neuron pathway from the ventral tegmental area (VTA) to the nucleus accumbens (NAc) is non-myelinated and unaffected by short-term enhanced neuronal activity in the young mouse brain
- P2. Pinjala, S.,** Biology
Chemogenetic Manipulation of Indirect Pathway in Parkinson's Disease via Subthalamic Nucleus Compares Favorably to AAV-GAD Therapy
- P3. Wolf, M.,** Cellular & Molecular Neuroscience
Establishing the Effects of Alcohol on Human Induced Pluripotent Stem Cells (hiPSCs) and hiPSC-derived Human Cerebral Organoids (hCOs)
- P4. Lua, E.,** Biology
The Impact of Cigarette Smoke and Ethanol Co-exposure on Mice
- P5. Passarelli-Roberts, L.,** Cellular & Molecular Neuroscience
Efficacy of Ketamine to Regulate eEF2 in Female Mice
- P6. Dietz, N.,** Cellular & Molecular Neuroscience
Impact of IL-17a antibody treatment on heroin-induced IL-17a pathway signaling
- P7. Brubaker, T.,** Cellular & Molecular Neuroscience
Carbonic Anhydrase Inhibitors Promote Amyloid-Beta Clearance in Alzheimer's Disease Model
- P8. Szmanski, O.,** Cellular & Molecular Neuroscience
Effects of Troriluzole on Anxiety- and Depression-like Behaviors in Methamphetamine-Naive and Methamphetamine-Abstinent Mice
- P9. Forry, T.,** Cellular & Molecular Neuroscience
The Antinociceptive and Analgesic Effects of Mitragynine and Cannabinoids in Two Mouse Pain Models
- P10. Bulusu, B.,** Cellular & Molecular Neuroscience
Cannabinoid modulation of opioid induced tolerance and withdrawal
- P11. Ansari, Y.,** Biology
Effectiveness and Safety of Endoscopic Neurotomy in Managing Chronic Low Back Pain: Comprehensive Systematic Review and Meta-Analysis of 440 Cases

- P12. Muruganandam, G.,** Cellular & Molecular Neuroscience
ZNF362 (Lin-29) as a Potential Therapeutic Target for Spinal Cord Injury Repair and Recovery
- P13. Balaji, S.,** Cellular & Molecular Neuroscience
Spinal cord axon regeneration through the inhibition of novel cytoskeletal protein
- P14. Zholdosh kyzy, K.,** Cellular & Molecular Neuroscience
Epigenetic changes in development of Myelomeningocele
- P15. Petraskaite, D.,** Cellular & Molecular Neuroscience
Investigating the Impact of 5-methylcytosine (5mC) and 5-hydroxymethylcytosine (5 hmC) on Alzheimer's Disease Pathogenesis
- P16. Kennelly, M.,** Biology
Women's Health and Aging Clocks: Ovarian Tissue-Specific DNA Methylation Age Predictions
- P17. Mercado, G.,** Cellular & Molecular Neuroscience
The Effects of Proximal vs. Distal Synaptic Transmission of Signals in Neural Circuitry
- P18. Arroyo, E.,** Biology
Development of Edible Films that Contain α -tocopherol
- P19. Oxenreider, O.,** Biochemistry
Preliminary Pharmaceutical Properties of CBD Oral Films
- P20. Mancner, I.,** Biology
Liposomes Interactions with Platelets via Fluorescence Spectroscopy
- P21. Vajipayajula, D.,** Cellular & Molecular Neuroscience
Investigating Y155 Phosphorylation of Protein Kinase C δ on Blood Platelets as a Model for Neuronal Disease Mechanisms
- P22. Siddiqui, F.H.,** Biology
Bmi1 Mediates Repair Post-Myocardial Injury by Modulation of Fibrosis
- P23. McDonnell, L.,** Biochemistry
Salmonid Myostatin Pathway Diversification as a Result of Whole Gene Duplication Events

- P24. Kabir, S.,** Biology
Targeting Talin-Induced Integrin Activity with Natural Product Molecules: A Potential Approach in Cancer Therapy
- P25. Harolika, R.,** Biology
Control of Metabolism by Ca²⁺ in Melanoma Progression
- P26. Patton, K.,** Biology
Sex differences in a mouse model of melanoma
- P27. Sahotra, S.,** Biology
Restoring pVHL interactions in mutant clear cell renal cell carcinoma with a small molecule
- P28. Satasiya, V.,** Biology
Characterization of novel effectors in the progranulin/EphA2 axis in bladder cancer
- P29. McCullough, L.,** Biology
WEE1 inhibition Synergistic targets
- P30. Chung, S.,** Biology
A Novel Multidomain Potts-Hamiltonian Model to Assess Substitution Rate Heterogeneity
- P31. Gallo, K.,** Genomic Medicine
A comprehensive comparison between evolutionary models in HyPhy and CODEML
- P32. Lange, V.,** Biology
Mitogenomic: Rates of Evolution of Passerine Birds
- P33. Le, A.,** Biology
Investigating Constraints on the Evolution of Floral Longevity in *Sabatia angularis*
- P34. Pan, J.,** Biology
From Theory to Practice: Hands-on Exploration of Environmental Resilience at Ambler Field Station
- P35. Engle, M.,** Biology
Ground Invertebrate Diversity in Varying Levels of Disturbance
- P36. Meinert, K.,** Biology
Invasive Pioneer Plant Species Presence in Differently Disturbed Temperate Old-Growth Forests

- P37. Anglin, M.**, Environmental Science
Understanding moss communities in temperate forest ecosystems following disturbance
- P38. Stoy, L.**, Ecology, Evolution & Biodiversity
Effect of Disturbance on the Composition of Mushroom Colonies Through Time
- P39. Brownfield, J.**, Ecology, Evolution & Biodiversity
When the time is right: Exploring potential niche partitioning of aquatic invertebrates in ephemeral ecosystems of a tornado-disturbed forest
- P40. Bucher, S.N.**, Biology
Exploring Invertebrate Species Composition Differences to Further Analyze Metacommunity of Ephemeral Pools
- P41. Brown, B.**, Biology
Standing Biomass's Effect on Seed Dispersal Patterns
- P42. Joseph H.**, Biology
SLF-GPT: Your Comprehensive Guide to Spotted Lanternfly Research
- P43. Becker, C.**, Biology
Effects of spotted lanternfly presence on parasitic Hymenoptera community composition

POSTERS
IN ALPHABETICAL ORDER

Effect of Standing Biomass on Seed Dispersal Dynamics in a Wind Disturbed Temperate Forest

Brian Brown, Chris LeClair, Katharine Stevenson, Dr. Mariana Bonfim, Dr. Amy Freestone
Temple Ambler Field Station • Temple University
Department of Biology • College of Science and Technology
brian.brown0004@temple.edu



Abstract

Seed dispersal is a crucial mechanism used in the dispersal of many biological organisms. The ability to disperse seeds is crucial to the success of a species, as germination by allowing seeds to travel away from their parent plant. In the summer of 2021, the oak-grove forest, TFO was hit by an EF-2 tornado, leaving behind a severely damaged forest. To understand how our forests are adapting to anthropogenic-driven climate change, it is important to understand how mechanisms, such as seed dispersal, are affected during the regeneration process. We collected data to compare the standing biomass (kg) in TFOs and Robbin Park's forest plots to the types of dispersal found in the collected seed rain. We found that standing biomass (kg) may not have as large an influence on seed dispersal as expected. Overall, understanding the mechanisms our forests use to regenerate is important to reduce forest loss due to climate-driven disturbances. This study will help us better understand how forests respond to natural disturbances.

Introduction

- In December of 2021, Temple's Forest Observatory (TFO) experienced a tornado that destroyed many of the previously standing biomass (kg).
- Wind disturbances can increase heterogeneity of a forest (Curtis et al., 2018).
- Disturbances can affect the composition of a forest by changing forest structure (Laurance & Garcia, 2020).
- Seed dispersal is essential for recovery after a disturbance (Bakker et al., 1996).
- Types of dispersal found at TFO and RBP:
 - Animal
 - Wind
 - Ballistic
- Hypothesized that wind dispersal will be observed at higher rates than animal dispersal in areas that have less standing biomass (kg).**
- Hypothesized that RBP will have less wind dispersed seeds than TFO due to it being undisturbed**

Methods

- Collect seeds from wind traps at different sites: TFO, disturbed & Robbin Park, disturbed & Robbin Park.
- 5 seed traps per quad, 18 quads in TFO & 6 quads in Robbin Park (n=120 seed traps)
- Collected seeds routinely

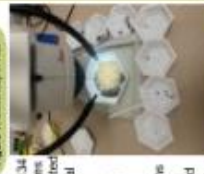


Figure 1: Seed trap in RBP

- Identified 30,134 seeds to a species level and separated them by dispersal type using a dissecting microscope and seed guide
- Created graphs to compare variations in seed dispersal type to standing biomass (kg)



Figure 2: Seeds guide identified by species

Results

Location	Animal	Wind	Ballistic	Animal and Wind	Total
TFO	23044	481	822	882	25009
RBP	4759	82	0	304	5125
BOTH	27783	563	822	1186	30134

Table 1: The total number of seeds collected at each location, separated by dispersal type

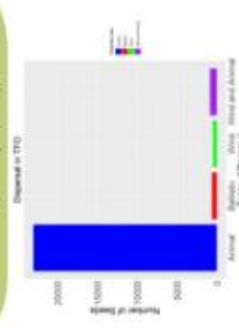


Figure 3: Number of seeds collected in TFO, separated by dispersal type

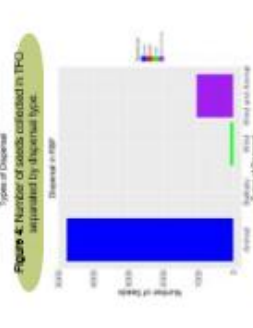


Figure 4: Number of seeds collected in RBP, separated by dispersal type



Figure 5: Number of seeds compared to biomass (kg) of total plots at Temple Field Observatory

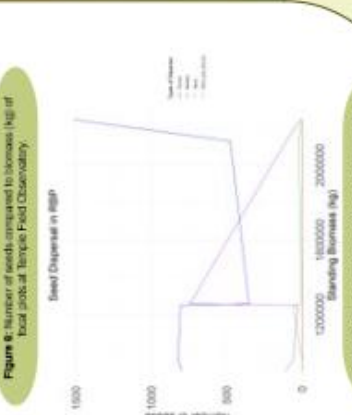


Figure 6: Number of seeds compared to biomass (kg) of total plots at Robbin Park

Top Seed of Each Dispersal Type

- Liriodendron tulipifera** (Wind & animal dispersed)
- Impatiens capensis** (Ballistically dispersed)
- Phytolacca americana** (Animal dispersed)
- Erechtites hieracifolius** (Wind dispersed)

Future Research

- Investigate if seasonality has any influence on the data collected
- Examine how invasive species may affect native seed dispersal
- Investigate how the understory affects seed dispersal patterns
- Determine the success rates of each type of dispersal

Acknowledgments: I would like to thank Chris LeClair and Katharine Stevenson for adding me through this process. I would also like to thank Dr. Bonfim and Mary Condon for their helpful inputs, as well as my fellow interns for assisting with field work.

Conclusions

- Both locations were composed of roughly the same percentage of wind dispersed seeds (Table 1).
- There were many more animal dispersed seeds collected in TFO than any other seed dispersal type (Fig. 4).
- TFO had 22,044 seeds of the invasive botanical species, *Phytolacca americana*
- In TFO, the abundance of animal seed dispersal decreased as standing biomass (kg) increased, while other types of dispersal remained relatively constant (Fig. 6)
- Phytolacca americana* might have better reproduction success in areas with less standing biomass (kg).
- In RBP, the abundance of animal seed dispersal was greater than any other type and increased with standing biomass (kg) (Fig. 7).
- Seed dispersal by animals might be the most effective dispersal method in undisturbed forests.
- The opposing trend of animal dispersed seeds and standing biomass (kg) in sample size between TFO and Robbin Park may have been caused by each site having a different dominant species or by the difference in sample size between the locations.
- This data shows that standing biomass (kg) may not play a major role in seed dispersal and instead specific forest traits, such as species makeup may play a bigger role in shaping seed dispersal dynamics in a forest ecosystem.

Introduction

- As proteins evolve, the rate of substitution varies across amino acid positions
- Previous studies consider invariant sites to best describe variable rates (compared to single-rate (S) or Gamma-distributed (Γ) models) observed in protein evolution (Fig. 1)
- Current protein evolution models use direct coupling analysis (DCA) approaches to infer evolution in a single domain across homologous proteins
 - These models cannot address variable substitution across a biologically realistic protein sequence, which has multiple domains

We hypothesize that variable rates across amino acid sites are due to coevolutionary interactions (epistasis) between multiple domains within a protein sequence.

Our proposed Joint Potts Model (JPM) simulates evolution across a tri-domain pseudo-protein while considering epistatic interactions between amino acid sites

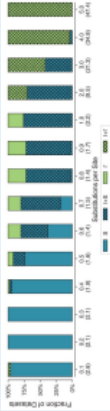


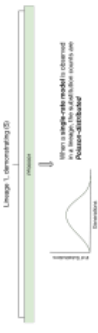
Fig. 1: The fraction of PFD0001 domains in which a given model is the best fit determined (Pati & Kumar, 2021)

H_1 : The number of substitutions across a protein with multiple domains will demonstrate a Poisson-distribution across amino acid sites.

H_2 : The number of substitutions across a protein with multiple domains will demonstrate a negative binomial distribution across amino acid sites.

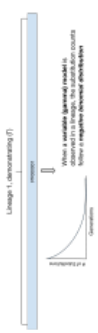
Fitting Probability Distributions to Rates

Poisson distribution of evolutionary events (H_1):



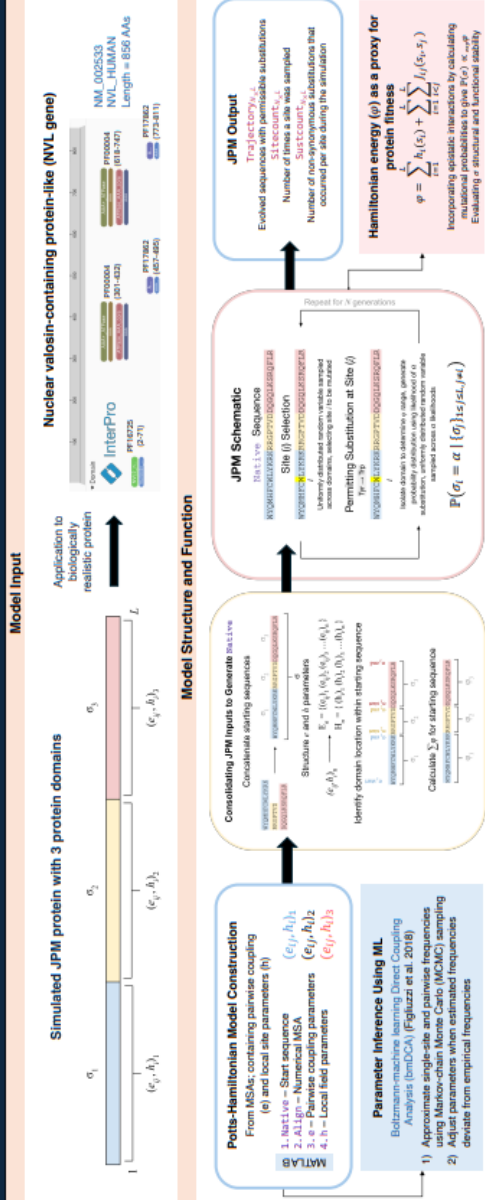
- Amino acid substitution is due to random fixation of nearly neutral or selectively neutral mutations
- Substitution events are isolated and occur at a constant rate (Kimura & Ohta 1971)

Negative binomial distribution of evolutionary events (H_2):

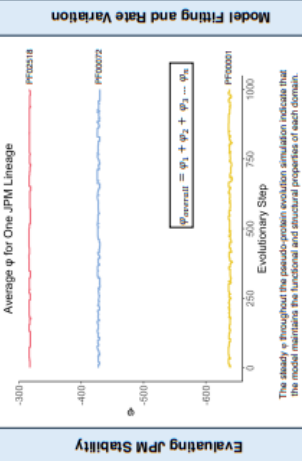


- Negative binomial distribution results from epistatic relationships occurring between evolutionary events and across amino acid positions
- Selective pressure on an amino acid varies among both position and evolutionary time (Uzuel & Corbin 1971)

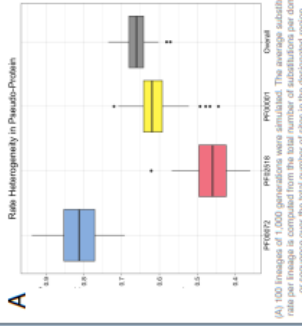
Joint Potts Model Framework



Results



The study throughout the results section includes simulation iterations that the model maintains the functional and structural properties of each domain.



(A) 100 lineages of 1,000 generations were simulated. The average substitution rate per lineage is computed from the total number of substitutions per domain or sequence over the total number of sites in the designated region.

(B) The fraction of lineages in which the substitution rate is best fitted to probability distribution model. Each lineage is composed of 1,000 generations of simulated data.

Conclusion

- Gamma-distributed rate variation is evident in lineages simulated from a synthetic protein with multiple domains
- A negative binomial distribution is present in some lineages
- JPM is capable of simulating protein evolution in biologically realistic complex proteins while preserving its structural and functional integrity.

Future Directions

- Analysis on biologically realistic complex proteins
- Optimization of model to parameterize the numbers of domains present in target protein sequence
- Widespread application of JPM to homologous proteins
- Determining the best fitting model for substitution rate heterogeneity that is uniformly applicable across proteins

References

- De La Paz et al. *PNAS* 2020, 117, 5873-5882.
- Patel & Kumar. *PNAS* 2021, 118, 18.
- Uzuel & Corbin. *Science*. 1971, 172, 1089-1096.
- Ohta & Kimura. *J Mol Evol*. 1971, 1, 18-25.
- Figliuzzi et al. *Mol. Bio and Evol*. 2018, 35, 1018-1027.

Impact of IL-17a antibody treatment on heroin-induced IL-17a pathway signaling



School of Medicine
TEMPLE UNIVERSITY

Nikki Dietz¹ and Dr. Stephanie E. Daws^{2,3}

¹College of Science and Technology, Temple University, Philadelphia, PA USA,
²Center for Substance Abuse Research, Temple University, Philadelphia, PA USA,
³Department of Neural Sciences, Temple University School of Medicine, Philadelphia, PA USA.
Correspondence: Stephanie Daws-Stephanie.Daws@temple.edu



Background and Introduction

In recent years, the misuse of heroin and other opiate medications has reached epidemic levels. Opioid-induced regulation of inflammation is a consequence of opioid use. Consequently, there has been interest in examining how various cytokines, specifically the interleukin-17 (IL-17) pathway, is affected by opioids such as heroin. IL-17a increases neuroinflammation, and thus reducing IL-17a signaling may reverse heroin-induced gene expression within the brain.

This study explores the impact of the IL-17a antibody on heroin-induced signaling of the IL-17a pathway in the prefrontal cortex in an experimenter-administered protocol of heroin and IL-17a combined exposure.

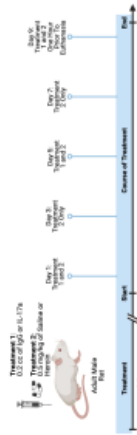
We hypothesize that co-treatment of rats with IL-17a antibody and heroin will result in blockade of heroin-induced inflammatory signaling in the rat brain. This project will determine whether IL-17a signaling aberrations caused by heroin are reversed with an IL-17a antibody and provide insight into whether the IL-17a antibody can impact brain gene expression when administered systemically.

Methods

The experiment was conducted using fifty-six adult male rats that were aged about 8 weeks old. Heroin hydrochloride was dissolved in 0.9% sterile sodium chloride at a dose of 0.5 mg/ml. Sterile sodium chloride was used as the control for heroin exposure and was administered in the same volume. The IL-17a antibody was administered at a dose of 0.2mg per rat in a volume of 200 μ l. An IgG antibody was used as a control for the IL-17a antibody exposure and was administered in the same volume (200 μ l).

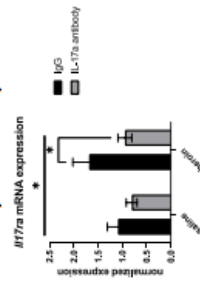
Over nine days, the rats were weighed and treated with specific treatments. The experimenter administered the IgG-saline, IgG-heroin, IL-17a-saline, and IL-17a-heroin. The experiment was performed in Fall 2023 with a first cohort and repeated in Spring 2024 with a second cohort to ensure reproducibility of results. The timeline of treatment is shown below.

Treatment Timeline



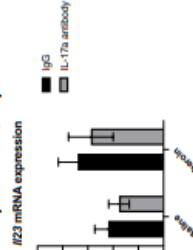
Results

Reduction of the IL-17 Receptor in IL-17a/Heroin Experimental Group



The qPCR findings showed that in comparison to the IgG/Heroin group of animals, the IL-17a animals had a significant reduction of the IL-17 receptor, and much less of the IL-17a receptor was expressed in the prefrontal cortex. A two way ANOVA revealed a significant main effect of antibody pretreatment on *Il17ra* expression, and a trend for a main effect of drug that did not reach statistical significance, with no drug by antibody pretreatment interaction. *Il17ra* expression in the heroin/IgG group tended to be higher than saline/IgG controls, although it did not reach statistical significance with a posthoc Tukey test. Further posthoc Tukey tests determined a significant reduction in *Il17ra* in the PFC of heroin/IgG-treated animals, compared to the heroin/IgG.

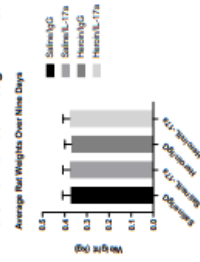
Levels of the IL-23 Receptor Remained Unchanged for All Experimental Groups



The qPCR findings revealed no significant change in the levels of *Il23* expressed in the PFC. There was not a large amount of variation of expression in all the treatment groups, and we cannot assume there was any change in the *Il23*. A two way ANOVA revealed no significant main effect of antibody pretreatment or drug on *Il23* expression, with no drug by antibody pretreatment interaction. *Il23* expression did not reach statistical significance with a posthoc Tukey test. Levels of *Il17ra*, *Ccl3* and *Il6* mRNA were below the limit of detection in the PFC. In the NAC, levels of genes of interest were below the level of detection.

Results Continued

Weights of Animals Maintained through All Treatments



Heroin exposure and IL-17a antibody treatment did not impact animal weight.

Conclusions

The IL-17a/Heroin animals displayed a significant reduction in the IL-17a receptor, meaning that the inflammatory cytokine, IL-17a, had less ability to interact with its receptor and induce IL-17a signaling cascades. This proinflammatory cytokine passes the blood-brain barrier and is shown to be elevated in individuals with opioid use disorders. However, we did not detect a significant difference in the downstream signaling molecule, IL-23, which is activated in response to IL-17a. Further studies to understand the impact of IL-17a antibody on IL-17a signaling pathways are warranted. Targeting the IL-17a pathway may be important for reducing heroin seeking behavior.

It was also observed in the NAC brain region that levels of all transcripts of interest were unable to be detected. We hypothesize that there are less IL-17 receptors in the NAC, which likely may mean that there is less impact of IL-17a antibody in this brain region. We would like to repeat this in the future in another study to understand the regulation of heroin in the NAC region and how various interleukin receptors may play a role. A more sensitive measure of gene expression may be required, such as digital PCR, or we may need to use a larger amount of starting mRNA material. The same is true for amplifying *Il6* and *Ccl3* mRNA in the PFC.

The misuse of opioids is steadily increasing in the United States. This study has shown to be stepping stone in understanding the complex interactions between drug-induced neuroadaptations and neuroinflammation. Combined with our *in vivo* functional studies, these findings are novel in the search for new pathways that may be targets to treat opioid seeking behavior.

Ground Invertebrate Diversity in Varying Levels of Disturbance

Mia Engle, Mary Cortese, Dr. Mariana Bomfim, Dr. Amy Eresztos
Temple Ambler Field Station • Temple University
Department of Biology • College of Science and Technology
Mae.engle@temple.edu



Five different species of ground beetles
Nicrophorus vespilloides
Dirt Covered Love Bug

Abstract

Insect diversity has been found to forest health, with healthier forests having an increase in diversity. Additionally, insects have been shown to be highly sensitive to environmental disturbance. In fall 2021, the Temple Ambler Field Station was hit by an EP2 tornado. To assess the impact of this disturbance, we conducted a study to assess the level of disturbance and subsequent changes in ground beetle diversity. We used pitfall traps to collect samples across sites with varying levels of disturbance during two different seasons. Data analysis has shown differences in community composition and diversity of invertebrates related to disturbance level. Some of the commonest found species in both and medium levels of disturbance include *A. bipunctata*, *O. rugosus*, and *L. bipunctatus*, which are part of the decomposer and predator families. We also saw changes in community composition with season, samples had an increase of spider species and an overall increase in abundance in the spring compared to fall. A comparative assessment of insects had never been completed for the Temple Ambler Field Station. This project seeks to understand how the insect community may be impacted due to the disturbance and whether there are seasonal trends to increase in frequency under climate change.

Background

- Invertebrates typically comprise 70%-90% of taxa and dominates animal biomass in forest ecosystems. Since they comprise such a large amount of the animal biomass, arthropods are essential for a functioning ecosystem.
- Arthropod diversity generally increases with forest age, time since prior disturbance, and the remaining area of forest.

Hypothesis:

In 2021 the Temple Forest Observatory (TFO) was hit by an EP2 tornado. After examining the level of disturbance, insect and ground invertebrate diversity is expected to decrease—losing species such as arboreal decomposers, predators and herbivorous invertebrates. Additionally, we expect to find an increase in decomposer species in areas of the forest with the highest levels of disturbance. With the changing seasons we expect to see more arthropod species like spiders and saw flies to be collected in the fall.

Methods

- Samples were collected using pitfall traps:
 - Covers were made with plastic board and nails to hold trap in place.
 - Traps were located in quadrats with varying levels of disturbance:
 - High: TFO 0306 and 0309
 - Medium: TFO 0112 and 0015
 - Low: Robbins park 0302 and 0303
 - Each quadrat had three traps.
 - Samples were collected weekly over a one-month period.
 - Each sample was processed by identifying and quantifying species.
 - Data was processed in R studio.
- 2 plastic cups dug into ground, one outer (210oz) with drainage holes and one inner (16oz) filled 1/4 of the way with water and dish soap.
- A funnel to prevent small mammal and herpetofauna bycatch (Photo to the right)



Results

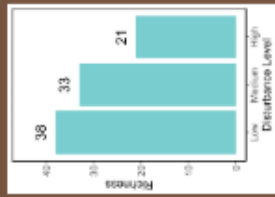


Figure 1: Species richness per disturbance level across seasons

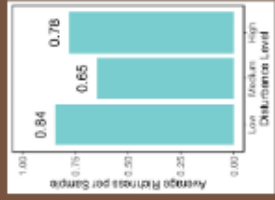


Figure 2: Average richness per sample across disturbance levels

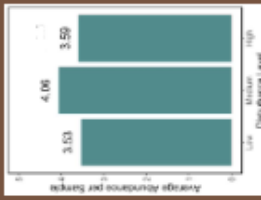


Figure 3: Total abundance of individuals per total individuals per site across disturbance levels

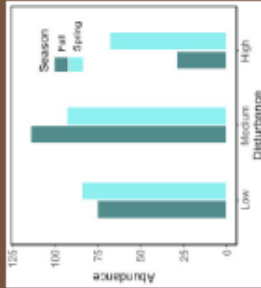


Figure 4: Average abundance of individuals per sample across seasons

Discussion

- Species richness per disturbance level shows low disturbance displaying the highest level of species richness at 38, the medium disturbance having the second highest species richness at 33, and the highest disturbance having species richness of 21 (Figure 1).
- When comparing for seasonal effects we found that the medium disturbance had the lowest number of species found in sampling (Figure 2).
- A higher richness in the low disturbance area can be attributed to the greater niche availability in a healthy undisturbed forest allowing for more species to colonize that habitat compared to the disturbed site.
- The total abundance of individuals across all disturbance levels shows that the medium disturbance has the highest number of individuals with 207, the low disturbance following with 159 individuals found, and high disturbance having lowest abundance with 97 individuals (Figure 3).
- When comparing for seasonal effects this system continued, with medium disturbance having the highest number of individuals in samples.
- We ran an ANOVA on our total abundance counts and found that disturbance level was insignificant (ANOVA $p = 0.1$, Figure 3).
- Highest abundance in medium disturbance levels (Figure 3) indicates a seasonal relation to the intermediate disturbance hypothesis with the medium disturbance showing highest abundance. In high disturbance areas the environment is unsuitable for many species leading to reductions in abundance.
- Another likely explanation for the higher abundance in medium disturbance would be a dominant species being *O. rugosus* (Figures 3 & 4). 17 individuals were found in the fall, but only in the medium disturbance, most likely meaning there was high abundance of animal feces (their main food source) around the traps.
- Trophic level richness shows that there was a high number of predator invertebrates in each level of disturbance. This is due to the high number of spiders found in the spring (Figure 5) that were not found in the fall.
- While there was no significant relationship between season and total abundance there was higher abundance in low and high disturbance sites in the spring (Figure 6). Higher spring abundance correlates with warmer temperatures and mating season.
- We found 24 new species in the spring that were



Figure 5: Average abundance of individuals per sample across seasons
Figure 6: Average abundance of individuals per sample across seasons
Figure 7: Average abundance of individuals per sample across seasons
Figure 8: Average abundance of individuals per sample across seasons
Figure 9: Average abundance of individuals per sample across seasons
Figure 10: Average abundance of individuals per sample across seasons
Figure 11: Average abundance of individuals per sample across seasons
Figure 12: Average abundance of individuals per sample across seasons
Figure 13: Average abundance of individuals per sample across seasons
Figure 14: Average abundance of individuals per sample across seasons
Figure 15: Average abundance of individuals per sample across seasons
Figure 16: Average abundance of individuals per sample across seasons
Figure 17: Average abundance of individuals per sample across seasons
Figure 18: Average abundance of individuals per sample across seasons
Figure 19: Average abundance of individuals per sample across seasons
Figure 20: Average abundance of individuals per sample across seasons
Figure 21: Average abundance of individuals per sample across seasons
Figure 22: Average abundance of individuals per sample across seasons
Figure 23: Average abundance of individuals per sample across seasons
Figure 24: Average abundance of individuals per sample across seasons
Figure 25: Average abundance of individuals per sample across seasons
Figure 26: Average abundance of individuals per sample across seasons
Figure 27: Average abundance of individuals per sample across seasons
Figure 28: Average abundance of individuals per sample across seasons
Figure 29: Average abundance of individuals per sample across seasons
Figure 30: Average abundance of individuals per sample across seasons
Figure 31: Average abundance of individuals per sample across seasons
Figure 32: Average abundance of individuals per sample across seasons
Figure 33: Average abundance of individuals per sample across seasons
Figure 34: Average abundance of individuals per sample across seasons
Figure 35: Average abundance of individuals per sample across seasons
Figure 36: Average abundance of individuals per sample across seasons
Figure 37: Average abundance of individuals per sample across seasons
Figure 38: Average abundance of individuals per sample across seasons
Figure 39: Average abundance of individuals per sample across seasons
Figure 40: Average abundance of individuals per sample across seasons
Figure 41: Average abundance of individuals per sample across seasons
Figure 42: Average abundance of individuals per sample across seasons
Figure 43: Average abundance of individuals per sample across seasons
Figure 44: Average abundance of individuals per sample across seasons
Figure 45: Average abundance of individuals per sample across seasons
Figure 46: Average abundance of individuals per sample across seasons
Figure 47: Average abundance of individuals per sample across seasons
Figure 48: Average abundance of individuals per sample across seasons
Figure 49: Average abundance of individuals per sample across seasons
Figure 50: Average abundance of individuals per sample across seasons
Figure 51: Average abundance of individuals per sample across seasons
Figure 52: Average abundance of individuals per sample across seasons
Figure 53: Average abundance of individuals per sample across seasons
Figure 54: Average abundance of individuals per sample across seasons
Figure 55: Average abundance of individuals per sample across seasons
Figure 56: Average abundance of individuals per sample across seasons
Figure 57: Average abundance of individuals per sample across seasons
Figure 58: Average abundance of individuals per sample across seasons
Figure 59: Average abundance of individuals per sample across seasons
Figure 60: Average abundance of individuals per sample across seasons
Figure 61: Average abundance of individuals per sample across seasons
Figure 62: Average abundance of individuals per sample across seasons
Figure 63: Average abundance of individuals per sample across seasons
Figure 64: Average abundance of individuals per sample across seasons
Figure 65: Average abundance of individuals per sample across seasons
Figure 66: Average abundance of individuals per sample across seasons
Figure 67: Average abundance of individuals per sample across seasons
Figure 68: Average abundance of individuals per sample across seasons
Figure 69: Average abundance of individuals per sample across seasons
Figure 70: Average abundance of individuals per sample across seasons
Figure 71: Average abundance of individuals per sample across seasons
Figure 72: Average abundance of individuals per sample across seasons
Figure 73: Average abundance of individuals per sample across seasons
Figure 74: Average abundance of individuals per sample across seasons
Figure 75: Average abundance of individuals per sample across seasons
Figure 76: Average abundance of individuals per sample across seasons
Figure 77: Average abundance of individuals per sample across seasons
Figure 78: Average abundance of individuals per sample across seasons
Figure 79: Average abundance of individuals per sample across seasons
Figure 80: Average abundance of individuals per sample across seasons
Figure 81: Average abundance of individuals per sample across seasons
Figure 82: Average abundance of individuals per sample across seasons
Figure 83: Average abundance of individuals per sample across seasons
Figure 84: Average abundance of individuals per sample across seasons
Figure 85: Average abundance of individuals per sample across seasons
Figure 86: Average abundance of individuals per sample across seasons
Figure 87: Average abundance of individuals per sample across seasons
Figure 88: Average abundance of individuals per sample across seasons
Figure 89: Average abundance of individuals per sample across seasons
Figure 90: Average abundance of individuals per sample across seasons
Figure 91: Average abundance of individuals per sample across seasons
Figure 92: Average abundance of individuals per sample across seasons
Figure 93: Average abundance of individuals per sample across seasons
Figure 94: Average abundance of individuals per sample across seasons
Figure 95: Average abundance of individuals per sample across seasons
Figure 96: Average abundance of individuals per sample across seasons
Figure 97: Average abundance of individuals per sample across seasons
Figure 98: Average abundance of individuals per sample across seasons
Figure 99: Average abundance of individuals per sample across seasons
Figure 100: Average abundance of individuals per sample across seasons



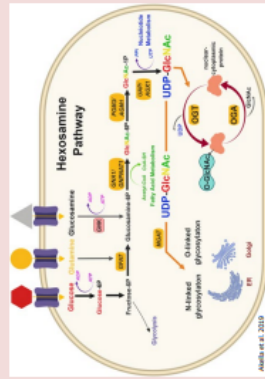
Control of Metabolism by Ca²⁺ in Melanoma Progression



SSP
SCIENCE SCHOLARS PROGRAM

N. Shamas¹, S. Gross¹, Ph.D., **Roban Harollikar²**, Adam Karami, AP Armistead¹, MIR Zaidi¹, Ph.D., J. Soboloff¹, Ph.D.,
¹Fels Institute for Cancer Research, Lewis Katz School of Medicine at Temple University, Philadelphia, PA-19140, USA
²Fox Chase Cancer Institute, Philadelphia, PA-19111, USA

Introduction



- Melanoma is the fifth most diagnosed cancer in the United States¹.
- Stress-oriented Ca²⁺ entry (SOCE) occurs when endoplasmic reticulum membrane protein STIM interacts with the plasma membrane Ca²⁺ channel Orai².
- Ca²⁺ signaling is known to modulate many key processes associated with tumor progression, including ER³ and metabolic reprogramming (such as activating key enzymes in the Krebs cycle⁴).
- Previous work showed that ultraviolet radiation (UVR) causes SOCE suppression, an elevation in glucose uptake without an increase in glycolysis or basal respiration.
- However, **this relationship between SOCE suppression and metabolism in melanoma is poorly studied.**
- RNA-seq analysis of SOCE suppressed cells and UVR exposed cells show upregulations in key enzymes associated with the hexosamine biosynthesis pathway (HBP), an important regulator of cell signaling favoring tumor formation⁵.
- The role of Calcium signaling and O-GlcNAcylation in melanoma remain elusive.

Results

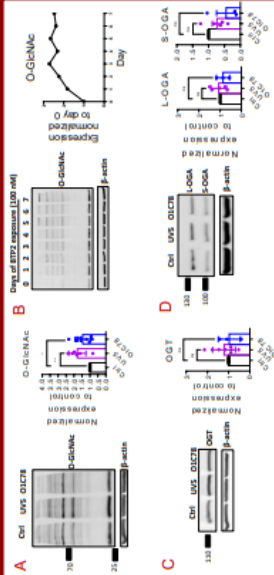


Figure 1: UV and SOCE suppression causes increased protein O-GlcNAcylation.

References:
1. Siegel, R. L., Miller, K. D., Fuchs, H. E., & Jemal, A. (2022). Cancer statistics, 2022. *CA: A Clinical Oncology Journal*, 72(1), 7-33.
2. Shamas, N., Gross, S., Karami, A., Harollikar, R., Armistead, A., Zaidi, M., Soboloff, J., & Shamas, N. (2023). Ultraviolet Radiation Suppresses SOCE and Increases O-GlcNAcylation in Melanoma. *Journal of Cellular Biochemistry*, 124(1), 1-12.
3. Shamas, N., Gross, S., Karami, A., Harollikar, R., Armistead, A., Zaidi, M., Soboloff, J., & Shamas, N. (2023). Ultraviolet Radiation Suppresses SOCE and Increases O-GlcNAcylation in Melanoma. *Journal of Cellular Biochemistry*, 124(1), 1-12.
4. Shamas, N., Gross, S., Karami, A., Harollikar, R., Armistead, A., Zaidi, M., Soboloff, J., & Shamas, N. (2023). Ultraviolet Radiation Suppresses SOCE and Increases O-GlcNAcylation in Melanoma. *Journal of Cellular Biochemistry*, 124(1), 1-12.
5. Shamas, N., Gross, S., Karami, A., Harollikar, R., Armistead, A., Zaidi, M., Soboloff, J., & Shamas, N. (2023). Ultraviolet Radiation Suppresses SOCE and Increases O-GlcNAcylation in Melanoma. *Journal of Cellular Biochemistry*, 124(1), 1-12.

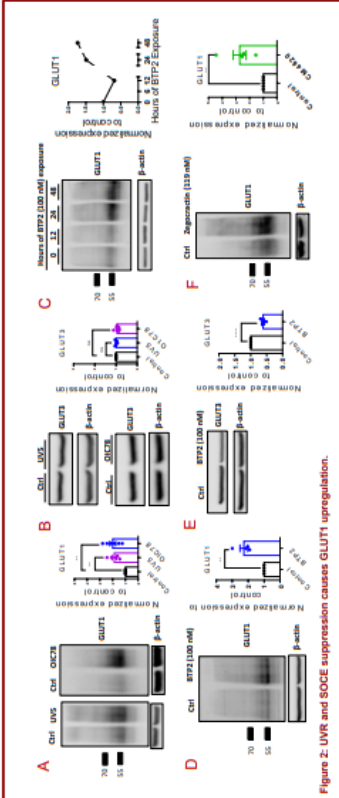


Figure 2: UVR and SOCE suppression causes GLUT1 upregulation.

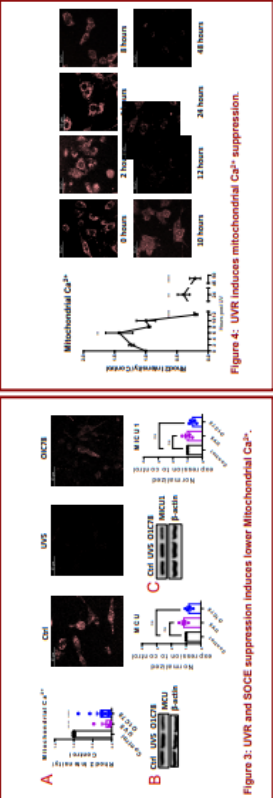


Figure 3: UVR and SOCE suppression induces lower Mitochondrial Ca²⁺.

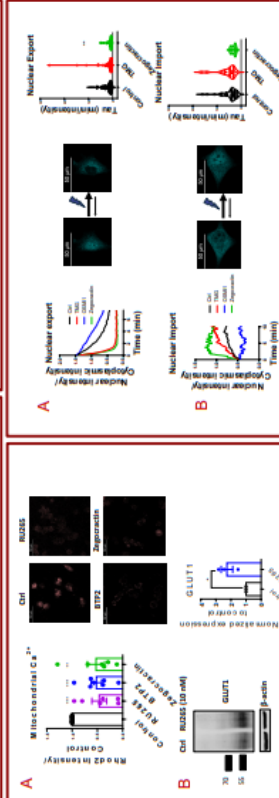


Figure 4: UVR induces mitochondrial Ca²⁺ suppression.

Figure 5: Mitochondrial Ca²⁺ suppression causes GLUT1 upregulation.

Figure 7: NUPs O-GlcNAcylation alters nuclear permeability.

Conclusions

SOCE suppression causes, mitochondrial Ca²⁺ suppression, then upregulation of GLUT1 followed by O-GlcNAcylation of proteins (nuclear pore proteins) that contribute to invasion

Acknowledgements: We would like to acknowledge Dr. Hsin-Yen Tsai (The Mblair Institute). This project was funded by 1R01CA15206, Research Summer 2022 and Summer 2022 funded by CARAS Grant.



SLF-GPT: Your Comprehensive Guide to Spotted Lanternfly Research

Hannah Joseph, Dr. Matthew R. Helmus
Integrative Ecology Lab, Department of Biology, Temple University



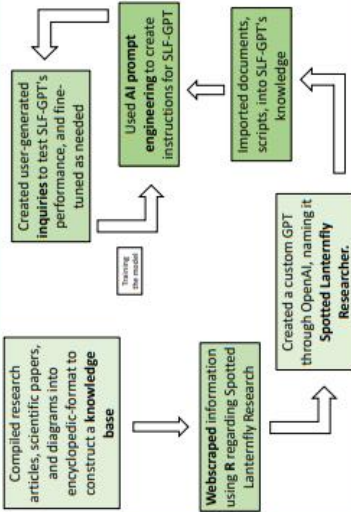
Abstract

Generative Pre-trained Transformers (GPT) have opened new ways in utilizing artificial intelligence as a tool in scientific research, processing a variety of information. The development of a GPT specialized for Spotted Lanternfly, *Lycorma delicatula*, research addresses the need for comprehensive and accessible knowledge for the general community. The Spotted Lanternfly GPT (SLF-GPT), is designed to assimilate vast amounts of data from scientific research papers and regulatory guidelines, offering insights into the biology, behavior, ecological impact, and control measures of this species. SLF-GPT enables users to understand complex scientific inquiries, provide detailed information, and suggest management strategies tailored to homeowners, vineyard operators, and forestry specialists. The GPT will incorporate peer-reviewed research papers and expert guidelines, ensuring it delivers accurate, relevant, and comprehensive responses. This project aims to bridge the gap between advanced scientific research and practical, actionable knowledge for combating this invasive species. By making scientific knowledge accessible to a broader audience, it will empower communities to practice more effective management practices, contributing to mitigate the impacts of this invasive species.

Introduction

- The spotted lanternfly, *Lycorma delicatula*, is an invasive polyphagous species native to parts of China, India, Vietnam and established in South Korea. The first detection was in Berks County, Pennsylvania, in 2014.
- Nymphs undergo four instars, as their appearance progressively changes while transforming into an adult, displaying a unique wing pattern with black spots on a gray forewing and vibrant red underwings.
- L. delicatula* polyphagous nature poses a significant challenge as they feed on the sap of more than 70 plant species, including Tree-of-Heaven (*Ailanthus altissima*).
- Management strategies are being developed, focusing on the combination of these methods to manage populations effectively while minimizing environmental impact.

Methods



References

Do, Z. et al., (2020). Global phylogeography and invasion history of the spotted lanternfly revealed by mitochondrial phylogenomics. *Evolutionary Applications*, 14(4), 915–930. doi.org/10.1111/evo.13170

Huron, N. A. et al., (2022). Pennsylvania severity assessment of a U.S. grape pest to disrupt the global wine market. *Communications Biology*, 5(1). doi.org/10.1038/s42003-022-02880-w

Julian, L. & Leach, M., (2023). Biology and Management of the Spotted Lanternfly, *Lycorma delicatula* (Homoptera: Psyllodea), in the United States. *Annual Review of Entomology*, 68(1), 153–187. doi.org/10.1146/annurev-ento-120220-111440

Generated Images of Spotted Lanternflies and Preferential Host (Tree-of-Heaven)



Generated Response of the Question: "How do Spotted Lanternflies affect ecosystems?"

How do Spotted Lanternflies affect ecosystems?

Spotted Lanternfly Researcher

The Spotted lanternfly (*Lycorma delicatula*) is an invasive pest with significant impact on ecosystems, primarily through its feeding behavior and the subsequent ecological effects. These insects feed on a wide variety of plants, including many trees, shrubs, and agricultural crops. Their feeding method and the effects on ecosystems can be summarized as follows:

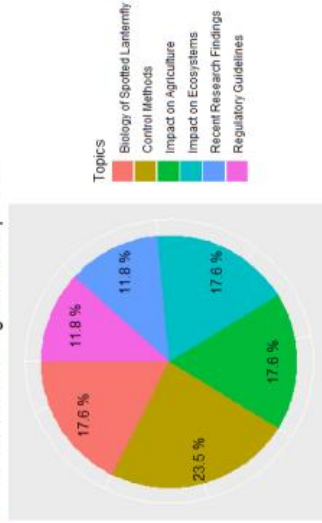
Feeding Damage: Spotted lanternflies feed by sucking sap from the phloem of plants using their piercing mouthparts. The feeding can stress plants, making them more susceptible to diseases and environmental stresses. In severe infestations, this can lead to the decline or death of the plants.

Novel Pest: As they feed, Spotted lanternflies excrete a sugary sticky product known as honeydew. This honeydew can cover plants and the ground beneath them, leading to the growth of sooty mold. Sooty mold can inhibit photosynthesis in plants by blocking sunlight, further stressing them and reducing their growth and vigor.

Attraction of Other Pests: The honeydew produced by Spotted lanternflies can attract other

Estimated Composition of SLF-GPT's Knowledge Base:

SLF-GPT Estimated Knowledge Base Composition



Discussion

- The results shown portrays the variety of ways of how SLF-GPT can produce a response to questions about *L. delicatula* research.
- The creation of SLF-GPT, specialized in spotted lanternfly research, represents an innovative intersection of AI technology and biodiversity.
- We are currently working towards training the model to generate descriptive and evidence-based responses for user-generated inquiries.
- By providing accurate, accessible information on this invasive species, SLF-GPT can play a crucial role in informing management strategies, supporting research efforts, and raising public awareness.

Acknowledgements

This project was funded by Temple University's Research Scholars Program within the College of Science and Technology, as well as IECOLab at Temple University under the supervision of Principal Investigator Dr. Matthew R. Helmus.



Targeting Talin-Induced Integrin Activity with Natural Product Molecules: A Potential Approach in Cancer Therapy

Salvin Kabir, Baihao Su, Jinhua Wu

Molecular Therapeutics Program, Fox Chase Cancer Center, Philadelphia, PA – 19111.



Abstract

This study investigates the impact of a group of natural product molecules on the specific interaction between integrin and its activator protein, talin, that mediates cellular adhesion, and derivatives of Cyanidin-3-galactoside chloride (C3G) via integrin peptide. Talin is instrumental in facilitating cell migration, invasion, and metastasis by engaging with integrin β subunits. Our investigation centers on the differential impacts of a group of natural product molecules related to Cyanidin-3-galactoside chloride (C3G), namely Cyanidin chloride (CC) and Pelargonidin chloride (PC), on the talin-integrin complex. Employing advanced protein expression and purification techniques along with fluorescence polarization assays, we investigated the binding affinities and inhibitory activities of these molecules on talin's functionality. Our findings reveal a compound-specific modulation of talin activity, where CC exhibits a marked influence on talin1 (Th1), and PC is more effective on talin2 (Th2). This specificity highlights the necessity of customizing therapeutic interventions to leverage distinct molecular interactions, paving the way for more targeted and efficacious cancer treatments. The insights gained from this study improve our understanding of talin's role in cellular processes and highlight its potential as a therapeutic target, advocating for a strategic approach in the development of new therapeutic agents targeting integrin-related diseases.

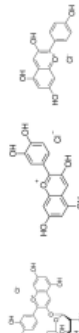


Fig 1: Structure of Cyanidin-3-galactoside (C3G) on the left, Cyanidin chloride in the middle, and Pelargonidin chloride on the right.

Talin structure

Talin is the most well-studied integrin activator. Two isoforms have been identified in vertebrates, Talin1 and Talin2. While shares 76% amino acid sequence identity, they are different in many aspects, such as expression pattern and function. Talin1, encoded by the *Tln1* gene, exists ubiquitously. Talin2, encoded by the *Tln2* gene, is abundant in the heart and brain but is expressed at lower levels in skeletal muscle, liver, and lung.

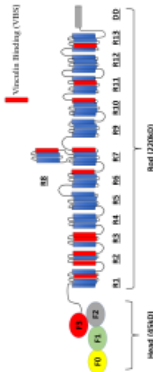
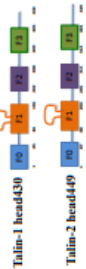


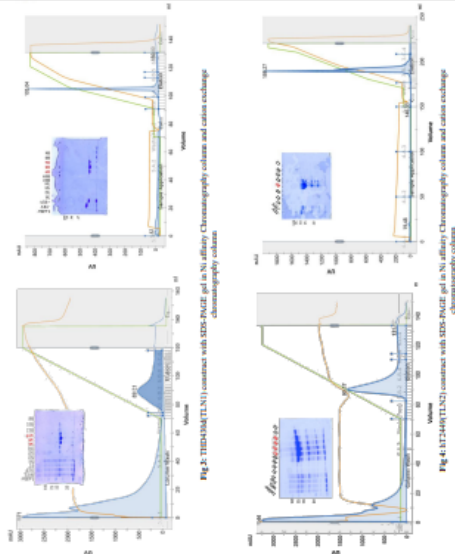
Fig 2: Visual depiction of talin FERM and RBD domains. Head domain (60-100), green (F1), grey (F2), and red (F3). Tail domain (200-260). Repeated Iys domains (R1-R2, R4-R7, R8-R11, R13). Viscerin binding site (VBS). A separate red rectangle. Dimerization domain (DD): A grey area at the end of the tail domain.

Talin Construct



To study the role of compounds in talin-integrin interactions, various talin-1 and talin-2 constructs were designed. Mutations or deletions were incorporated, indicated by dashed (without loop) and solid (with loop) lines.

Purification Results



The purified protein's molecular weight was then determined using SDS-PAGE, confirming its integrity. Finally, we employed a dialysis column for buffer exchange, preparing the protein for fluorescence polarization (FP) assays. This comprehensive purification protocol ensured the protein was of high purity and suitable for accurate FP analysis.

Fluorescence polarization (FP) assay

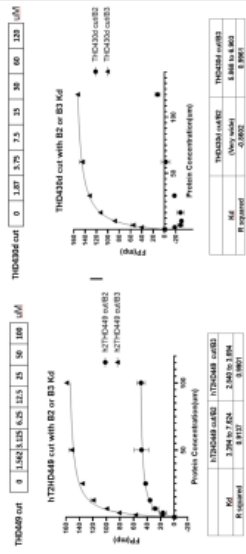
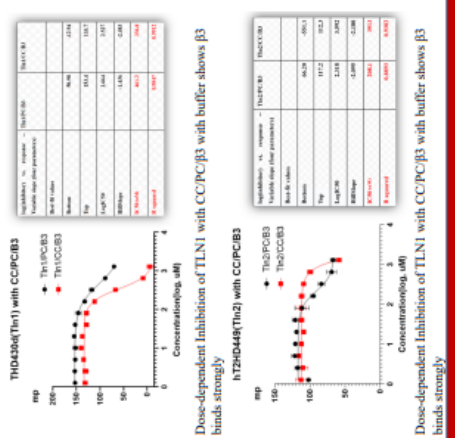


Fig 3: A control curve is generated to check the efficacy of the protein with $\beta 3$ peptide. $\beta 3$ peptide had a greater propensity for binding to both tested protein types. The consistent and strong binding of the $\beta 3$ peptide to two different protein constructions supports the idea that it has the potential to be a more effective binding partner in this biochemical environment. The higher R-squared values linked to the $\beta 3$ peptide interactions provide additional evidence supporting the accuracy and dependability of these findings.

Compound impact talin/integrin interaction



Dose-dependent Inhibition of TLN1 with CC/PC/ $\beta 3$ with buffer shows $\beta 3$ binds strongly

Conclusion

We have uncovered significant insights into the interactions and inhibitory potential of compounds CC and PC with talin proteins TLN1 and TLN2, revealing their selective efficacy in modulating these proteins' activity. CC showed superior inhibition of TLN1, highlighting its potential for targeted drug development by exploiting specific molecular interactions, especially under CC/ $\beta 3$ mimicking conditions. Conversely, TLN2 favored the interaction with PC, emphasizing the influence of the molecular environment on drug efficacy. The research also spotlighted the $\beta 3$ peptide's high affinity for both TLN1 and TLN2, suggesting a foundational role in designing peptide-based therapies targeting talin-mediated cellular processes. This investigation not only advances our understanding of talin's complex interaction with CC and PC but also opens new avenues for therapeutic interventions, underscoring the importance of tailoring drug design to specific protein interactions for more effective treatments.

Literature Cited

Zhang P, Azizi L, Kulkarni S, Gao T, Bakoglu M, Jacquier MC, Sun Y, Mizuta JAE, Cheng KH, Wehrle-Haller B, Hyman VP, Wu J. Crystal structure of the FERM-folded talin head reveals the determinants for integrin binding. Proc Natl Acad Sci U S A. 2020 Dec 22;117(51):32402-32412. doi: 10.1073/pnas.2014583117. Epub 2020 Dec 7. PMID: 33288722; PMCID: PMC7768682.

Acknowledgement

Thank you to the Diamond Research Scholar award for the funding and the amazing opportunity. I also wanted to thank you Jinhua Wu and fellow postdocs for all the help and facilities.



Mitogenomic: Rates of Evolution of Passerine Birds

Violet Lange¹, Maria Andreina Pacheco¹, Axel S. Cepeda¹, Miguel Lentino³, Ananias A. Escalante¹

¹Department of Biology/Institute for Genomics and Evolutionary Medicine (IGEM), Temple University, Philadelphia, PA-USA; ²Colectivo Ornitológica Phelps, Caracas, Venezuela



Abstract: Passeriformes are an order of the class Aves that includes all perching birds, which are characterized by the antitrochyl arrangement of their toes. This order makes up more than half of all extant bird species, which makes the study of passerine phylogenetics very important. Evolutionary biologists are heavily studying the phylogeny of this order due to its high morphological diversity and massive evolutionary radiation. Here, five new complete passerine mitochondrial genome (mtDNA) sequences are reported and aligned with 353 other passerine mtDNA sequences available in the GenBank using MAFFT software. Then, a maximum likelihood method was applied to estimate the phylogenetic tree using IQ-TREE software, and mtDNA sequences of closely related orders, including Falconiformes and Psittaciformes, were used as outgroups. Results were compared with previously published phylogenies using whole nuclear genomes. It was found that the phylogeny using mitochondrial genomes is consistent with previously reported phylogenies, with few discrepancies due to a lack of genome availability (sampling) or modifications to taxonomy. ReTime, a software that estimates evolutionary rates of species at every branching point on the tree, was implemented to approximate the rate of divergence of passerines. The evolutionary rates of the order Passeriformes will be discussed, and in the future, this phylogeny will be used to analyze the divergence times of passerine families.

Introduction

The order Passeriformes is composed of the most diverse grouping of birds from the class Aves. These species differ greatly in characteristics such as plumage, body structure, and song, and in social behavior, such as ecological roles and nesting systems. Due to about 60% of all bird species being passerines, they are at the forefront of ornithological research.

The phylogeny of birds is very complex and controversial and has yet to be fully resolved. This is due to the high rates of molecular evolution. Many researchers have used mtDNA to study relationships between members of this order is complicated and not yet completely resolved.

Objective: The objective of this phylogenetic analysis of passerines is to obtain mitochondrial genomes of not yet published species, resolve the relationships between the members of this order, and estimate divergence rates.

Results

Data from only 93 of 140 well-known families were available and recovered from GenBank for this analysis.

Genome sampling was improved by including data from five species with previously unavailable mitochondrial genomes.

Most of our mitochondrial genome phylogenetic tree matched the already published nuclear genome phylogenetic tree, with few discrepancies that attributed to species sampling.

As seen in previous studies, the mebeba, phylogeny of Passeriformes recovered suborders (Cyanini) and others (Passeri) as monophyletic groups, with the family Acridinidae being their sister group. The monophyly and relationship among these groups within Passeriformes have been well established using whole-genome nuclear data, including nuclear and more mitochondrial genomes.

About 50 families were estimated to have accelerated rates, which makes up about 45% of all the families used in this analysis.

Conclusion and Future Remarks

With this preliminary tree, we aim to improve the phylogeny of the most complex order of birds and continue to compare the consistency of phylogenies using nuclear and mitochondrial genomes.

We also will analyze the families with the fastest rates to determine if there is a correlation between the diversification and key characteristics such as distribution, coloration, and/or size.

We are interested in understanding how mitochondrial genomes diverge, evolution, and the phylogenetic tree will be used to estimate the divergence times for each family.

Methods

DNA Extraction

100 µl of blood was collected in 1.5 ml tubes (Eppendorf tubes).

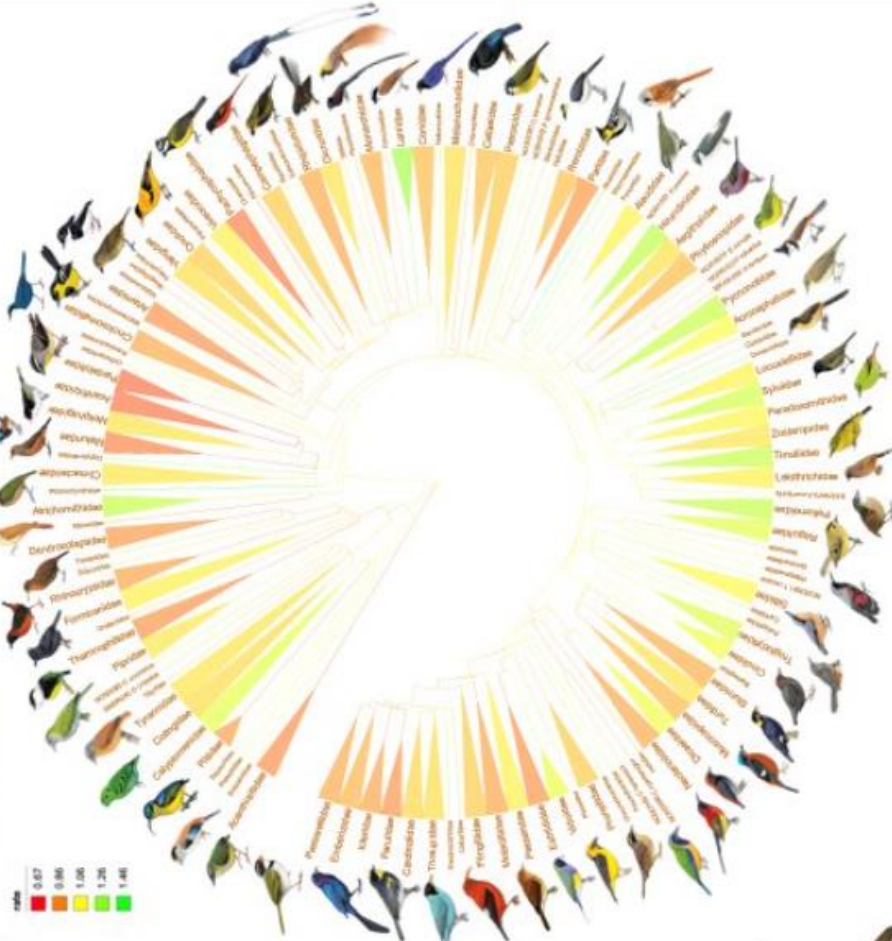
Data Collection

Alignment of Genomes (MAFFT)

353 Passerine Genomes

Mitochondrial Phylogenetic Tree

Rates and ReTime for rate estimations on tree



The impact of cigarette smoke and ethanol co-exposure on mice

Esmeralda Lua^{1,2}, Zoe M. Davis-Luitzer^{1,2}, Hassan Hayek^{1,2}, Karim Bähmed^{1,2,3}, Ellen Unterwald^{4,5}, T. K. Eisenstein^{4,5}, Beata Kosmider^{1,2,3}

¹Department of Microbiology, Immunology, and Inflammation, Temple University, Philadelphia, PA, ²Center for Inflammation and Lung Research, Temple University, Philadelphia, PA 19140, ³Department of Thoracic Medicine and Surgery, Temple University, Philadelphia, PA 19140, ⁴Department of Neural Sciences, Temple University, Philadelphia, PA 19140, ⁵Center for Substance Abuse Research, Temple University, Philadelphia, PA 19140

Abstract

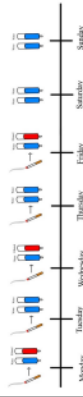
The most prevalent forms of substance abuse involve tobacco, in the form of cigarette smoking, and alcohol consumption, in the form of ethanol. However, the impact of the co-exposure in relation to lung injury is not widely understood or researched. The trajectory of the experiments outlined herein aims toward understanding the impacts of this co-abuse through examining gender differences of mice exposed to cigarette, ethanol, and co-exposed to cigarette smoke and ethanol. Smoking was administered for 2 hours at the same time every day, 5 days a week for 4 weeks. Following exposure to cigarette smoke, 10% ethanol was provided in the enclosure for approximately 21 hours. A statistically significant difference was observed in males, revealing heightened DNA levels in the plasma following exposure to cigarette smoke (CS) and ethanol. In contrast, females exhibited elevated GPC6 and GRM7 gene expression in response to cigarette smoke and ethanol exposure. Analysis of male and female mice also showed a decrease in mitochondrial DNA after cigarette smoke and ethanol exposure. Notably, a pronounced decline in female mice was detected, suggesting an impact on mitochondrial function in this group. Furthermore, protein expression was analyzed by Western blotting to define a pro-inflammatory response in murine lung tissue. Understanding the combined effects of cigarette smoke and alcohol consumption on lung injury is important to advance our knowledge of lung disease pathophysiology. It also aids in fostering the development of innovative therapeutics targeting respiratory dysfunction.

Aim

To understand the impacts of cigarette smoking on ethanol consumption and assess the combined effects of cigarette smoking and ethanol exposure on lung injury.

Methods

28-days old male and female mice C57/BL6 were used (Jackson Laboratory). The groups are as follows: air and water (Air + H₂O), air and ethanol (Air + EtOH), cigarette smoke and water (CS + H₂O), cigarette smoke and ethanol (CS + EtOH). Mice were exposed to cigarette smoke for 2 h/day at the same time everyday 5 days a week for 4 weeks. For ethanol groups, 10% ethanol was provided after exposure to cigarette smoke for 21 hours.



Mon., Wed., Fri.: Water Measurement
Tues., Thurs., Sat.: EtOH Measurement

Results
Increased DNA concentration in plasma obtained from males exposed to ethanol and CS

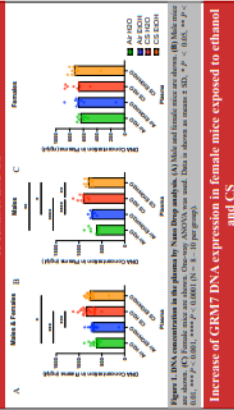


Figure 1. DNA concentration in the plasma by Western Blot analysis. (A) Males had significantly higher DNA concentration in plasma for males exposed to ethanol and CS. (B) Males had significantly higher DNA concentration in plasma for males exposed to ethanol and CS. (C) Males had significantly higher DNA concentration in plasma for males exposed to ethanol and CS. ANOVA was used. Data is shown as mean ± SD. **P* < 0.05, ***P* < 0.01, ****P* < 0.001 (N = 8-10 per group).

Figure 2. GRM7 DNA levels in plasma by qPCR. (A) Males and female mice are shown. (B) Males mice are shown. (C) Females mice are shown. (D) Males and female mice are shown. (E) Males mice are shown. (F) Females mice are shown. ANOVA was used. Data is shown as mean ± SD. **P* < 0.05, ***P* < 0.01, ****P* < 0.001 (N = 8-10 per group).

Figure 3. FGFR2 DNA levels in plasma by qPCR. (A) Males and female mice are shown. (B) Males mice are shown. (C) Females mice are shown. (D) Males and female mice are shown. (E) Males mice are shown. (F) Females mice are shown. ANOVA was used. Data is shown as mean ± SD. **P* < 0.05, ***P* < 0.01, ****P* < 0.001 (N = 8-10 per group).

Figure 4. GPC6 DNA levels in plasma by qPCR. (A) Males and female mice are shown. (B) Males mice are shown. (C) Females mice are shown. (D) Males and female mice are shown. (E) Males mice are shown. (F) Females mice are shown. ANOVA was used. Data is shown as mean ± SD. **P* < 0.05, ***P* < 0.01, ****P* < 0.001 (N = 8-10 per group).

Figure 5. Ethanol and CS has a small effect on the expression of GPC6 in female mice. (A) Males and female mice are shown. (B) Males mice are shown. (C) Females mice are shown. (D) Males and female mice are shown. (E) Males mice are shown. (F) Females mice are shown. ANOVA was used. Data is shown as mean ± SD. **P* < 0.05, ***P* < 0.01, ****P* < 0.001 (N = 8-10 per group).

cGAs and STING protein analysis in the lung tissue obtained from male and female mice exposed to ethanol and CS

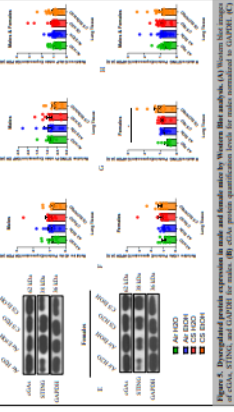


Figure 6. Dysregulated protein expression in male and female mice by Western Blot analysis. (A) Western blot images showing protein levels for cGAs, STING, and other markers. (B) Bar graphs showing protein levels for cGAs, STING, and other markers. (C) Bar graphs showing protein levels for cGAs, STING, and other markers. (D) Bar graphs showing protein levels for cGAs, STING, and other markers. ANOVA was used. Data is shown as mean ± SD. **P* < 0.05, ***P* < 0.01, ****P* < 0.001 (N = 8-10 per group).

Figure 7. IL-8 and IL-6 protein analysis in the lung tissue obtained from male and female mice exposed to ethanol and CS

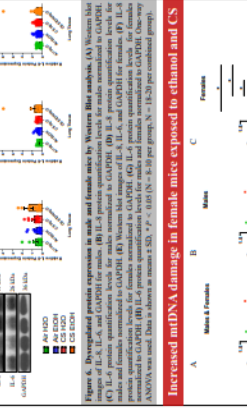


Figure 8. IL-8 and IL-6 protein analysis in the lung tissue obtained from male and female mice exposed to ethanol and CS. (A) Western blot images showing protein levels for IL-8 and IL-6. (B) Bar graphs showing protein levels for IL-8 and IL-6. (C) Bar graphs showing protein levels for IL-8 and IL-6. (D) Bar graphs showing protein levels for IL-8 and IL-6. ANOVA was used. Data is shown as mean ± SD. **P* < 0.05, ***P* < 0.01, ****P* < 0.001 (N = 8-10 per group).

P-IRF3 and IRF3 protein analysis in the lung tissue obtained from male and female mice exposed to ethanol and CS

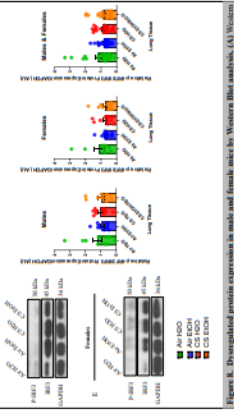


Figure 9. Dysregulated protein expression in male and female mice by Western Blot analysis. (A) Western blot images showing protein levels for P-IRF3 and IRF3. (B) Bar graphs showing protein levels for P-IRF3 and IRF3. (C) Bar graphs showing protein levels for P-IRF3 and IRF3. (D) Bar graphs showing protein levels for P-IRF3 and IRF3. ANOVA was used. Data is shown as mean ± SD. **P* < 0.05, ***P* < 0.01, ****P* < 0.001 (N = 8-10 per group).

Decreased mtDNA amount in both genders and increased mtDNA damage in female mice exposed to ethanol and CS

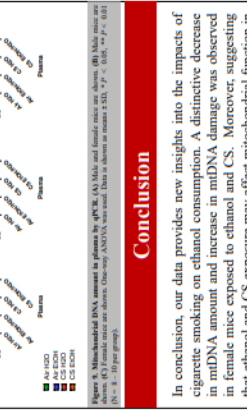


Figure 10. Mitochondrial DNA amount in plasma by qPCR. (A) Males and female mice are shown. (B) Males mice are shown. (C) Females mice are shown. (D) Males and female mice are shown. (E) Males mice are shown. (F) Females mice are shown. ANOVA was used. Data is shown as mean ± SD. **P* < 0.05, ***P* < 0.01, ****P* < 0.001 (N = 8-10 per group).

Conclusion

In conclusion, our data provides new insights into the impacts of cigarette smoking on ethanol consumption. A distinctive decrease in mtDNA amount and increase in mtDNA damage was observed in female mice exposed to ethanol and CS. Moreover, suggesting that ethanol and CS exposure may affect mitochondrial function in females.

Funding

This study was funded by the Pilot Project from National Institute on Drug Abuse Grant P30 DA013429 (E. Unterwald and T.K. Eisenstein)

Invasive Pioneer Plant Species Presence in Differently Disturbed Temperate Old-Growth Forests

Kelly Meinert*, Christopher LeClair, Mariana Bonfim, Mary R. Cortese, Amy L. Freestone, Brent J. Sewall

Temple Ambler Field Station • Temple University
Department of Biology • College of Science and Technology
*kelly.meinert@temple.edu



Abstract

On September 1st, 2021, Temple University's Ambler Campus was hit by a tornado (with highly destructive 130 mph wind speeds) that was brought upon by the remnants of Hurricane Ida. This large-scale wind disturbance provided a unique opportunity to study invasion by numerous previously absent non-native herbaceous and woody understory plant species. The goal of this project was to determine whether the composition, abundance, richness, and distribution of these invasive pioneer plants into areas of two old-growth forests that experienced different impacts of the tornado had a relationship to relative disturbance levels. A visual percent cover survey of 13 focal invasive pioneer species was performed in the summer of 2023. Preliminary results hint at overall invasive species abundance and richness being higher at the disturbed forest site (TFO) than at the undisturbed forest site (RBP). These findings are significant because these competitive interactions that non-native herbaceous layer may end up dominating the initial successional stages of the disturbed forest, potentially altering the composition and regeneration of the dominant overstory tree species in the disturbed forest.

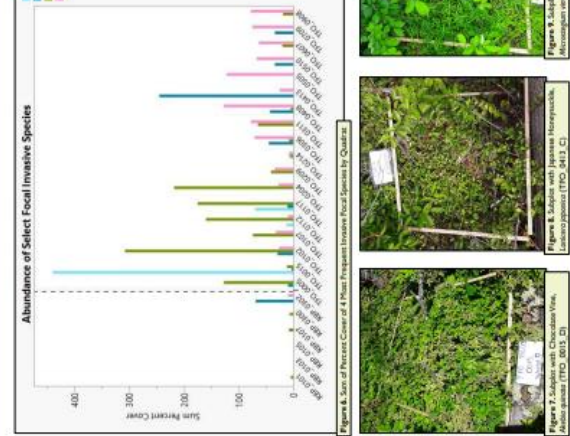
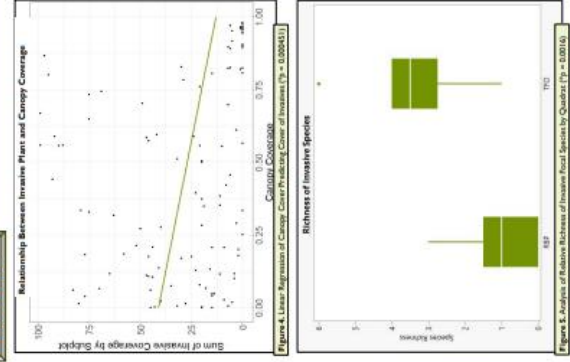
Introduction

- The invasion of introduced plants into natural communities is one of the most serious threats to biodiversity [1]
- Disturbance events may facilitate invasions by eliminating competitors or increasing resources [2]
- At the Temple Forest Observatory (TFO), hundreds of trees were either uprooted or destroyed by the 2021 tornado
- The nearby Robbins Park Environmental Education Center (RBP) was entirely unaffected by the tornado, providing a control, comparison undisturbed site (that largely resembles TFO before the tornado)
- Goal:** To determine whether the composition, abundance, richness, and distribution of invasive pioneer understory plant species is related to the level of disturbance in areas of two old-growth forests that experienced different impacts of a recent, large-scale wind disturbance

Methods

- Invasive Pioneer Focal Species Percent Cover**
- 5 (1m x 1m) subplots were constructed in each of the 24 (20m x 20m) focal quadrats, split between both research sites, for a total of 120 subplots
- 18 focal quadrats in the Temple Forest Observatory (TFO)
- 6 focal quadrats in Robbins Park Environmental Education Center (RBP)
- Visual estimates of percent cover for each of the 13 invasive focal species were assessed in the field
- The 13 invasive focal (herbaceous and woody) species were selected based on their known or suspected presence at either of the two sites
- Data was collected during the summer peak growing season (June-July 2023)

Results



Discussion & Future Directions

- Overstory percent canopy cover appears to predict percent cover of understory invasives (Figure 4)
- There is significantly higher invasive species richness at the TFO site than at the RBP site (Figure 5)
- Rubus phoeniculus* (Wineberry), *Microstegium vimineum* (Japanese Siltgrass), and *Lonicera japonica* (Japanese Honeysuckle), and *Akebia quinata* (Chocolate Vine) are the four most abundant invasive pioneer plant species present in TFO, with different species present across different areas (Figure 6)
- What are the next steps for this project?**
 - Using data derived from Image-Pro Premier Software analysis, adopt a "disturbance index" from overstory percent canopy cover values calculated from pictures taken directly over each of the 120 subplots
 - Further analyze the relationship between percent disturbance and percent invasion, looking for a potential trend
 - Using ArcGIS Pro Software, create both a comprehensive map of the localized invasions present at both sites and a map detailing the relative disturbance levels present across both sites

Acknowledgements: We would like to thank all the summer 2023 field station interns and technicians for their available data collection efforts, guidance and moral support. Anna Cooney, Beth Carroll, Lisa Chen, Grace Gorman, Sammie Jack, Cole Blackstock, Marissa Jones, and the Robbins Park Field Station staff for their help in this project and for providing me this amazing opportunity. Dr. Brent Swick, Dr. Amy Freestone, Dr. Mariana Bonfim, Mary Cortese, Kase Stevenson, and Chris LeClair. Special thanks to Matthew Cortese for his assistance in both field and office settings and appreciation for the College of Science and Technology Research Scholars Program.

References:
1. Davis, M. H. (1995). Global patterns of plant invasions and the impact of disturbance. *Ecology*, 76(1), 1252-1263.
2. Davis, M. H., Gibson, J. R., & Thompson, S. (2000). Invasional ratchets in plant communities. *Journal of Ecology*, 88(1), 528-534. <https://doi.org/10.1046/j.1365-2745.2000.00513.x>

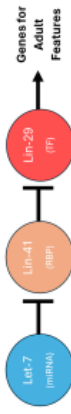
ZNF362 (Lin-29) as a Potential Therapeutic Target for Spinal Cord Injury Repair and Recovery

Ganesh Muruganandam, Ha Neui Kim, Shuxin Li

Shriners Hospitals Pediatric Research Center, Department of Neural Sciences, Lewis Katz School of Medicine at Temple University, Philadelphia, PA 19140, USA.

Introduction

Spinal cord injuries (SCIs) often result in permanent paralysis by severing nerve fibers in the corticospinal tract (CST).¹ This damage is mostly irreparable as mature neurons in the mammalian central nervous system (CNS), theoretically, cannot regrow their axons, although they can do so during development.² No treatment exists that can greatly improve SCI outcomes, but strategies targeting the genes regulating neuronal growth to stimulate axon regeneration may serve as a promising avenue for recovery.² ZNF362 (Lin-29) is a gene encoding a zinc finger transcription factor that promotes adult-specific tissue expression in *C. elegans* and possibly mammals.³ It participates in the Let-7/Lin-41 heterochronic developmental pathway, which is also thought to modulate neuronal growth capacity and suppress it after maturation in *C. elegans*.⁴



In this project, we examined Lin-29 as a potential molecular target for treating SCIs. We investigated whether inhibiting Lin-29 in CST neurons would promote axon regrowth and functional recovery after SCI using Lin-29 cKO and WT mouse models.

Methods

- Genetically modified CSTB1/6 mice with loxP sites flanking the Lin-29 gene were developed to utilize the Cre/loxP conditional knockout mechanism.
- SCIs were generated in adult mice (8-10 weeks old) from the developed strain as dorsal over-hemisections at the T7 vertebrae.
- 5 days after SCI, AAV vectors with GFP/Cre expression plasmids were injected into the sensorimotor cortices of experimental group mice to knock out Lin-29 in select CST neurons (Lin-29 cKO group). AAV vectors with GFP-only expression plasmids were injected into the same areas in control group mice (WT group).
- Open-field BMS was rated 2 hours and 2 days post-SCI, and weekly after. Grid walk, grasping, and narrow beam tasks were conducted 6 and 8 weeks post-SCI.
- 6 weeks after SCI, BDA neuron tracer was injected into the same AAV injection sites on the sensorimotor cortices of Lin-29 cKO and WT mice to trace CST neurons.
- Mice were perfused at 8 weeks post-SCI. Histological analysis was performed on spinal cord sections around the injury site. Axons regenerated caudal to the lesion site were quantified from manual axon tracings on software after imaging.

Data and Results

Inhibition of Lin-29 May Promote Axonal Regrowth in Adult Mice with Spinal Cord Injury

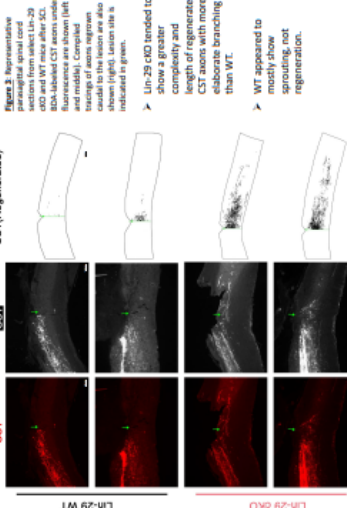
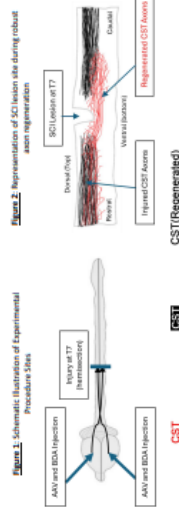


Figure 1. Schematic illustration of experimental procedures. **Figure 2.** Representative sections from WT and Lin-29 cKO mice after SCI. **Figure 3.** Comparison of total length of regenerated CST axons caudal to the lesion in Lin-29 cKO and WT mice after SCI at 8-week intervals.

Inhibition of Lin-29 May Promote Functional Recovery in Adult Mice with Spinal Cord Injury

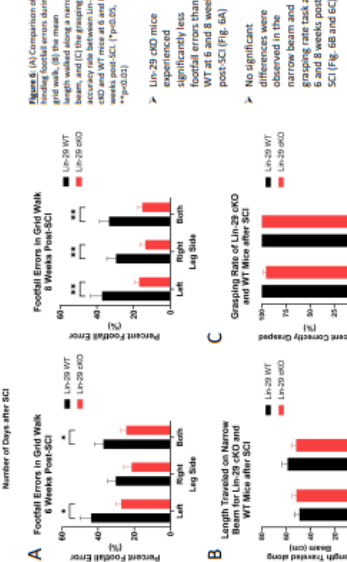
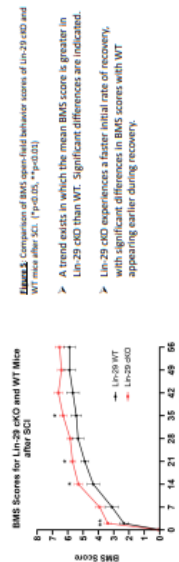


Figure 3. Comparison of BMS open-field behavior scores of Lin-29 cKO and WT mice after SCI. **Figure 4.** Comparison of footfall errors during grid walk. **Figure 5.** Comparison of length traveled on narrow beam, and (C) the grasping accuracy rate between Lin-29 cKO and WT mice at 6 and 8 weeks post-SCI.

References

1. Minamide, T. (2022). Mechanisms of Axon Growth and Regeneration. *Neuroscience and Biomedicine*. The Journal of Neuroscience, The Official Journal of the Society for Neuroscience, 42(16), 5885-5900.
2. Minamide, T., et al. (2020). Spinal cord injury: a review of current therapies, future treatments, and basic science findings. *Neuroscience Research*, 88(1), 1-10.
3. Minamide, T., et al. (2019). Identification of a novel transcription factor, ZNF362, that regulates axon growth and is expressed in the CNS. *Development*, 146(1), 1-10.
4. Minamide, T., et al. (2018). ZNF362, a novel transcription factor, regulates axon growth and is expressed in the CNS. *Development*, 145(1), 1-10.

Acknowledgements

This work was supported by the National Institutes of Health (NIH) (R01NS113267) and the Lewis Katz School of Medicine at Temple University (LKSOM) (R01NS113267).

Discussion and Conclusion

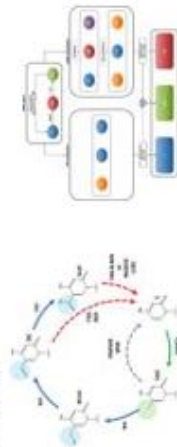
- Knocking out Lin-29 from CST neurons may contribute to stimulating axon regeneration in injured adult CST neurons and promoting functional recovery after SCI.
- Lin-29 cKO had a greater potential for regenerative axon regrowth, which is better for SCI repair.³
- Knocking out Lin-29 may have a greater impact in improving initial SCI recovery. It may also enable a better long-term recovery for some functions compared to others.
- Lin-29 may be involved in regulating the intrinsic growth capacity of mammalian CNS neurons, making it a potential molecular target for treating SCIs through regenerative methods.
- Lin-29 is conserved, and it may serve the same regulatory function in human CNS neurons.
- Targeting Lin-29 alone may not be enough to regenerate injured axons and promote recovery. A strategy that involves many other genes in addition to Lin-29 may be more effective for treating SCIs.
- Gene-modulating therapies that target the various intrinsic factors that heavily suppress CNS neuronal growth potential may be potent in treating SCIs and other conditions involving axon injury like stroke.

Abstract

Alzheimer's disease (AD) stands as a significant cause of both mortality and dementia, with existing treatments mainly focused on symptom management rather than altering the disease's trajectory. This study delves into the epigenetic intricacies of AD by exploring the roles of 5-hydroxymethylcytosine (5hmC) and 5-methylcytosine (5mC), which have shown promise as biomarkers for shedding light on AD's pathology. Leveraging advanced statistical and visualization techniques in Python to conduct a secondary analysis of the GSE109627 dataset (tissue: middle temporal gyrus), we identified unique methylation patterns in AD compared to control brain tissues. Our findings highlight marked epigenetic disparities that align with AD's progression, suggesting these modifications play a key role in the disease's underlying mechanisms. While acknowledging the study's limitations, such as sample diversity and conversion methodologies, we underline the significance of methylation and hydroxymethylation in understanding AD. This research points to an encouraging path for future therapeutic interventions. It emphasizes the necessity for further investigations with more diverse and extensive datasets to solidify the role of epigenetic modifications as AD biomarkers. In doing so, it lays a groundwork for subsequent studies aimed at deciphering AD's complexities, contributing significantly to the field of precision medicine in managing neurodegenerative diseases.

Background

In investigate the impact of 5-methylcytosine (5mC) and 5-hydroxymethylcytosine (5hmC) on Alzheimer's disease, we explore cytosine modifications crucial for gene regulation. DNA methyltransferases modify cytosine to 5mC, affecting gene suppression, while TET enzymes convert 5mC to 5hmC, potentially modulating gene expression. Distinguishing these modifications, Bisulfite Sequencing (BS) identifies unmethylated cytosines by converting them to uracil, but cannot differentiate between 5mC and 5hmC. Oxidative Bisulfite Sequencing (oxBS) advances this by specifically oxidizing 5hmC, enabling differentiation of 5mC and 5hmC. The difference in methylation levels detected by BS and oxBS (BS-oxBS) quantifies 5hmC, providing insights into Alzheimer's pathogenesis through epigenetic landscapes.

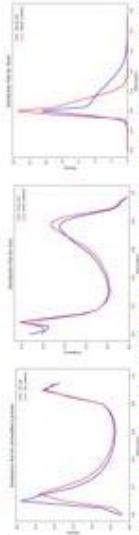


References

Landwehr B, Bocklandt K, Petersen J, et al. Alzheimer's disease-associated hypoxymethylation changes in the brain and blood. *Chin Epigenet* 11, 104 (2019). <https://doi.org/10.1038/s41437-019-0153-9>
Kovalevich, M, et al. (2017). Target specificity of oxBS for 5mC, 5hmC and 5fC. *Epigenetics and Chromatin* 10, 1-10 (2017).

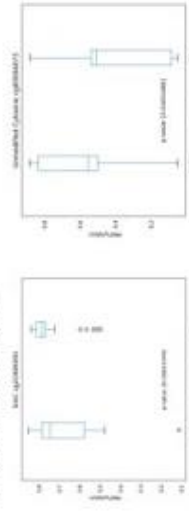
Results

Methylation Density in AD vs. Control across Cytosine Variants
Comprehensive analysis through three distinct line charts, each illustrating the density distribution of unmethylated cytosine, 5-methylcytosine (5mC), and 5-hydroxymethylcytosine (5hmC) were done. Notably, the density distribution for 5hmC showcases significant differences between AD and control groups. In the initial segment of the 5hmC line chart, AD samples exhibit a markedly lower methylation density compared to the control group. This suggests a potential hypomethylation state in the AD genome at specific regions which could be indicative of dysregulated gene expression associated with disease pathogenesis. Conversely, in the latter part of the chart, AD samples surpass the control in methylation levels, hinting at a shift to hypermethylation. This biphasic pattern of methylation in AD, starting with hypomethylation followed by a region-specific hypermethylation, may reflect a complex epigenetic modulation mechanism that contributes to Alzheimer's disease progression.



Comparative Analysis of Methylation Patterns: Unmodified Cytosine and 5mC

Comparative analysis of methylation patterns between unmethylated cytosine and 5-methylcytosine (5mC) in Alzheimer's disease (AD) pathogenesis was conducted. Two box plots were generated as examples to illustrate methylation levels of specific CG sites in AD versus control samples to illustrate methylation levels of 5mC. Statistically significant differences were observed in methylation levels between AD and control groups ($p < 0.05$), indicating a potential role of DNA methylation in AD development.



5hmC CG Sites and Associated Genes in Alzheimer's Disease Pathogenesis

In our study on Alzheimer's disease, we conducted an analysis to identify the top 200 5hmC CG sites and their associated genes.

Notably, prominent among these were PRM1, U2AF2, A1P53, C6orf47, ZNF467, TAF12, CLP1M1 and ISM1. These genes play crucial roles in various cellular processes implicated in Alzheimer's pathogenesis. Our findings shed light on potential molecular mechanisms underlying the disease, offering new avenues for therapeutic exploration.

Gene	AD	Control
PRM1	1.000000	1.000000
U2AF2	1.000000	1.000000
A1P53	1.000000	1.000000
C6orf47	1.000000	1.000000
ZNF467	1.000000	1.000000
TAF12	1.000000	1.000000
CLP1M1	1.000000	1.000000
ISM1	1.000000	1.000000
...

Differential Methylation Patterns in Alzheimer's Disease: A Comparative Analysis with Healthy Controls

When analyzing the methylation status of cytosine and its modified forms, 5-methylcytosine (5mC) and 5-hydroxymethylcytosine (5hmC), distinct patterns of methylation changes emerge. For unmethylated cytosine, there's a predominant loss of methylation in 58.5% of the instances, with a gain in 41.5% of cases, indicating a more frequent demethylation process.

In contrast, 5mC shows a significant trend towards methylation gain in 78% of cases, compared to a 22% loss, suggesting a strong inclination towards increased methylation. On the other hand, 5hmC predominantly undergoes demethylation, with a 68.7% loss and only a 31.2% gain in methylation.



Future Direction

Future research endeavors could build upon the findings of this study by exploring dynamic trajectories of epigenetic markers in Alzheimer's disease progression. Investigating potential biomarkers for early detection and monitoring holds promise for advancing diagnostic and therapeutic strategies. Furthermore, deeper exploration of 5hmC levels across CpG islands and samples could provide valuable insights into the underlying molecular mechanisms of Alzheimer's disease pathology.

Restoring pVHL interactions in mutant clear cell renal cell carcinoma with a small molecule

Sarah Sahotra¹, Mariam Fouad Hafez², John Karanicolas³

¹Biology Department, Temple University, Philadelphia, PA
²Cancer Signaling and Microenvironment Program, Fox Chase Cancer Center, Philadelphia, PA

Introduction

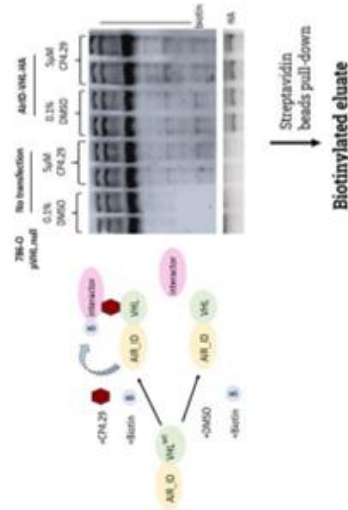
ccRCC is caused by mutations in a gene called VHL, which leads to the production of faulty or non-functional VHL proteins causing mutations like missense mutations. These mutated proteins are unable to carry out their normal functions, which can result in the development of tumors and other medical problems.

This study aims to explore VHL interaction with other proteins in ccRCC after treatment with the newly designed mutant pVHL refoldr CP4-29.

Methods

AirID experiment was used to identify VHL interactions in renal cancer cells, followed by AlphaFold modeling of these interactions for structural analysis.

AirID proximity biotinylation labelling and mass spectrometry profiling elucidated the pVHL interactome. AlphaFold2 facilitated structural modeling of up-regulated and down-regulated proteins.



CP4-29 reactivated the interactions of missense mutant pVHL

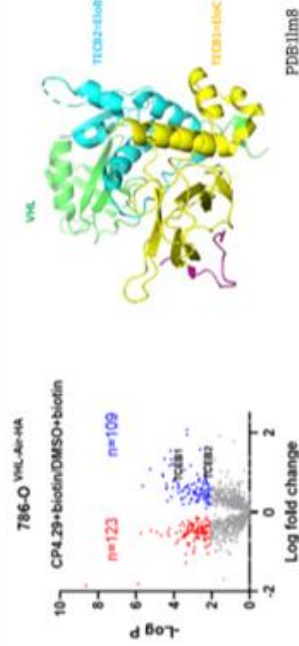


Figure 1. The up- and down-regulated proteins in 786-O renal cancer cells upon transfection with the biotinylating plasmid of Air-ID_VHL and mutant VHL.refolder molecule CP4-29.

VHL_SRP9_rank_002

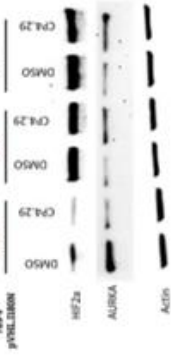


Figure 2. Machine learning scores for the AF2 generated models of protein interactions with VHL.

Figure 3. One of the top five interactor protein, SRP9 (turquoise) that has alpha docking to VHL (green)

Conclusion

- CP4-29 induced VHL interaction with its endogenous interactors, ELoB and ELoC, and a newly identified partner SRP9.

Acknowledgements

- Glenn Doyle
- Igor Bychkov
- Shabnam Pirestani
- Robert Broadrup
- Sven Miller
- Victoria Mischley
- Grigori Andrianov

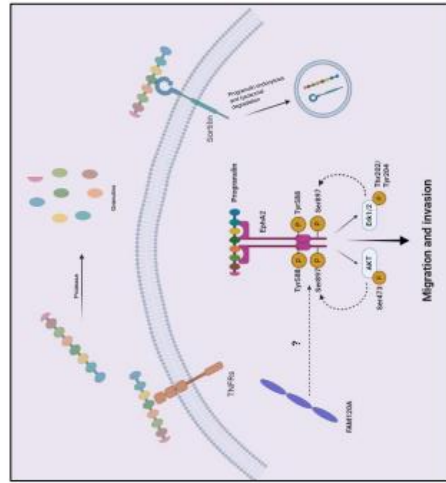
Vrunda Satasiya, Sharon Burk, Antonio Giordano, Andrea Morrione

Sbarro Institute for Cancer Research and Molecular Medicine, Center for Biotechnology, Department of Biology, College of Science and Technology, Temple University

Abstract

Bladder cancer is one of the most common malignancies, and it represents the ninth most common cancer diagnosis in the world. It is associated with substantial morbidity and mortality due to the burden of treatment and the cost of care for this malignancy. Progranulin is a pluripotent growth factor whose dysregulation is implicated in several human pathologies including frontotemporal dementia, inflammation, immune response and cancer. In bladder cancer, progranulin pro-tumorigenic action is mediated by the activation of its receptor, EphA2, a member of a large family of receptor tyrosine kinases, as in fact, we previously discovered that progranulin stimulates EphA2 phosphorylation at Ser897, which leads to enhanced tumor cell motility, invasion, and *in vivo* growth. We also demonstrated that EphA2 depletion significantly diminished progranulin-dependent motility and anchorage-independent growth, while enhancing sensitivity of bladder cancer cells to cisplatin treatment.

In recent years, the progranulin/EphA2 axis has emerged as a critical pathway in bladder cancer progression, but the molecular details of action are still poorly defined. We recently conducted mass spectrometry analysis and identified novel progranulin-dependent EphA2 interactors including FAM120A, which is a protein with a putative role in oncogenic pathways. We discovered that FAM120A is significantly expressed in urothelial carcinoma-derived cells. Importantly, we also demonstrate the EphA2 complexes with FAM120A in progranulin-dependent manner. Moreover, using immunofluorescence analysis we showed that EphA2 and FAM120A colocalized upon progranulin stimulation. Overall, this research offers insights into the progranulin/EphA2 signaling axis and uncovers new effectors for a better understanding of bladder cancer progression.



Objective

- > To investigate the basal expression levels of FAM120A in all urothelial carcinoma-derived bladder cancer cell lines.
- > To investigate whether EphA2 interacts with FAM120A upon PGRN stimulation.
- > To demonstrate whether EphA2 and FAM120A colocalize using immunofluorescence analysis.

Results

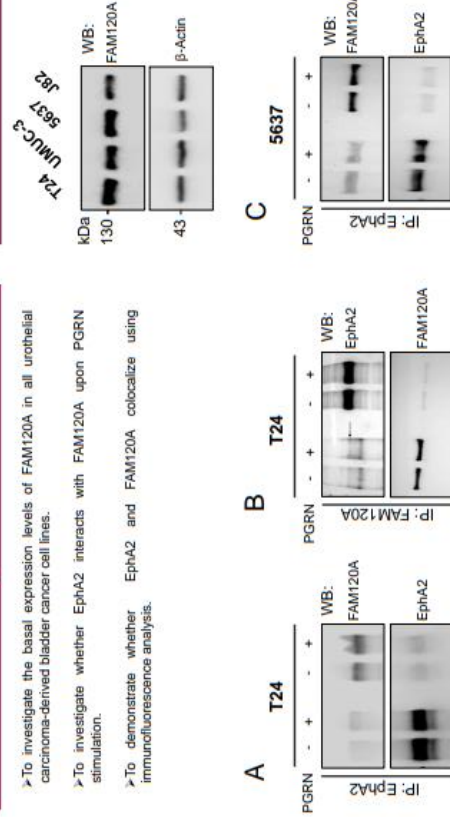


Figure 1. Expression level of FAM120A in different urothelial carcinoma-derived cell lines as detected by immunoblot with specific antibodies. Cell lysates were loaded on gel, transferred, immunoblotted with anti-FAM120A antibody at 4°C, and image was obtained through bright 1500.

Figure 2. Co-immunoprecipitation (Co-IP) of EphA2 and FAM120A. (A) T24 cells were serum-starved for 24 hours and then stimulated with progranulin at 100 nM for 15 minutes. Lysates were pre-cleared and immunoprecipitated with anti-EphA2 antibodies. Proteins were detected using anti-FAM120A via immunoblotting. (B) T24 cells were serum-starved and stimulated with progranulin as described in (A). Lysates were pre-cleared with protein A-Agarose beads and immunoprecipitated with anti-FAM120A. Proteins were detected using anti-EphA2 via immunoblotting. (C) Co-IP analysis was performed as described in (A) in 5637 cells.

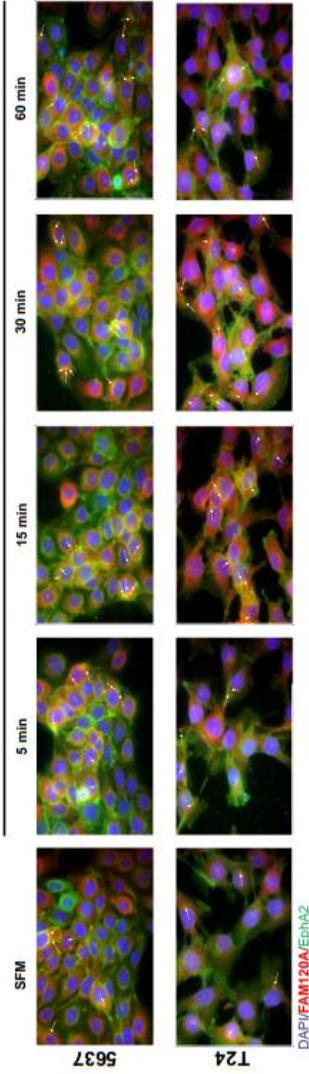


Figure 3. Progranulin modulates the colocalization EphA2 and FAM120A. 5637 and T24 cells were serum-starved for 4 hours and then treated with 100nM progranulin at indicated timepoints and stained for FAM120A and EphA2. Arrow points to the colocalization areas in different fields.

Conclusion

- > colli
- de
- ca.
- hlab...

Acknowledgement

- > This experiments were supported by the funds from Sbarro Health Research Organization. I wish to thank Dr. Antonio Giordano for his support and Dr. Andrea Morrione for his continuous invaluable guidance.



Trorilzole Reduces Methamphetamine-Induced Depression-like Behavior and Locomotor Sensitization in Mice

Ola Szmactinski¹, Sonita Wialer¹, Samhitha Reddy³, Megha Varghese¹, Jordyn Chambers¹, Scott Rawls²
¹College of Science and Technology, Temple University, Philadelphia, PA; ²Center for Substance Abuse Research, Lewis Katz School of Medicine at Temple University, Philadelphia, PA; ³College of Liberal Arts, Temple University, Philadelphia, PA



CENTER FOR
SUBSTANCE
ABUSE
RESEARCH

Background

- There is no FDA-approved treatment for psychostimulant use disorder.
- Dysregulation of glutamatergic mesocorticolimbic networks is associated with drug dependence.
- Glutamate contributes to behaviors induced by methamphetamine (METH) dependence such as depression, anxiety, and locomotor sensitization.
- Trorilzole (TRLZ) is the prodrug of riluzole (RLZ), a drug currently on the market for amyotrophic lateral sclerosis (ALS). TRLZ bypasses some metabolic and pharmacokinetic limitations associated with RLZ.
- TRLZ reduces glutamate transmission in two ways: by reducing neuronal glutamate and by enhancing astrocytic glutamate reuptake.
- TRLZ, via its unique, dual mechanistic action, has the potential to effectively regulate glutamatergic neurotransmission and normalize the behaviors of mice: following chronic METH exposure.

Methods

- **Subject:** Adult male C57Bl/6 mice
- **A 10-day METH and TRLZ binge** study was performed. The two-by-two study design is illustrated in Figure 1. Mice were given TRLZ (8 mg/kg) injections 15 minutes before METH (3 mg/kg) injections each day.
- **The Forced Swim Test (FST)** assay was used to test depression-like behavior in the mice. The FST assay was performed 72 hours after the conclusion of the binge. Mice were placed in glass, cylindrical tanks of water and remained in the water for 6 minutes.
- **The Elevated Plus Maze (EPM)** assay was used to test anxiety-like behavior in the mice. The EPM assay was performed 24 hours after the conclusion of the binge. Mice were placed in a maze with two "open" arms and two "closed" arms in the shape of a plus sign. Each mouse was allowed to roam for 5 minutes.
- **The Locomotion Assay** was used to test METH sensitization in the mice. The assay was performed 6 days after the conclusion of the binge. Baseline locomotor activity was recorded for the first 60 minutes. Each mouse was injected with METH (3 mg/kg) at the 60-minute mark. Locomotor activity was recorded in 5-min bins for 120 minutes.

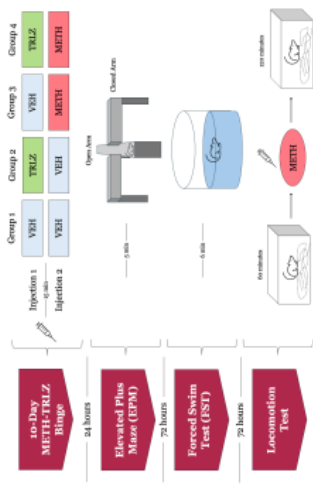


Figure 1 Summary of Methods. VEH= Vehicle with sterile water, TRLZ= Trorilzole at 8 mg/kg, METH= Methamphetamine at 3 mg/kg

Results

- Repeated TRLZ administration does not produce an anxiolytic effect after chronic METH exposure in mice. There were no significant increases in time in and entries into the open arms or decreases in time in and entries into the closed arms in the elevated plus maze (EPM) (Fig. 2, A-D).
- Repeated TRLZ administration reduces METH-induced depression-like behavior in mice in the forced swim test (FST). The immobility times of TRLZ-treated groups, compared to VEH-treated groups, were significantly lower when compared to METH-dependent mice (Fig. 3).
- Repeated TRLZ administration reduces locomotor sensitization caused by acute METH. Increases in ambulatory activity (Fig. 4A) and stereotypic activity (Fig. 4B) following METH injection were significantly reduced in the TRLZ-treated groups.

Discussion & Conclusions

- It was expected that TRLZ would reduce the anxiety-like behavior that emerges during METH withdrawal. The lack of anxiolytic effect by TRLZ may be explained by too short of an abstinence period to establish true METH withdrawal. Additionally, the EPM assay has previously shown contradictory results in measuring METH withdrawal-induced anxiety-like behaviors.
- TRLZ has the potential to treat a major negative symptom of METH withdrawal: depression. The depression that arises from METH abstinence is a significant contributor to relapse risk. By reducing the risk of relapse, TRLZ can treat and prevent METH dependence.
- Increased behavioral sensitization to acute METH is an indicator of increased drug cravings. In reducing the ambulatory activity of mice following METH injection, TRLZ showed the potential in reducing METH craving, which also has implications for relapse risk.

Future Direction

- A repeat study using female mice can address any potential sex differences in how TRLZ and METH are tolerated and affect behavior.
- Psychostimulant addiction is also associated with neuroimmune dysregulation, which contributes to dependence and relapse. A follow-up study is currently underway to study how TRLZ impacts the neuroimmune system via the modulation of cytokine levels, and how this neuroimmune modulation is correlated with the behavior-effects demonstrated in the present study.

References

- Alford, G. C., Merson, D. K., & Mink, A. M. (2011). Chemokines, cytokines and cell adhesion in drug and alcohol dependence. *PLoS*, *6*(10), e24824. <https://doi.org/10.1371/journal.pone.0024824>
- Alford, G. C., Merson, D. K., & Mink, A. M. (2012). Chemokines, cytokines and cell adhesion in drug dependence. *Journal of Psychiatric Research*, *46*(1), 1-10. <https://doi.org/10.1016/j.jpsychres.2011.07.005>
- Alford, G. C., Merson, D. K., & Mink, A. M. (2013). Chemokines, cytokines and cell adhesion in drug dependence. *Journal of Psychiatric Research*, *47*(1), 1-10. <https://doi.org/10.1016/j.jpsychres.2012.07.005>
- Chang, K. C., Yoon, K., Robinson, A. E., & Koob, G. F. (2011). Methamphetamine and amphetamine induce neuroimmune activation in the nucleus accumbens. *Journal of Neurochemistry*, *116*(1), 1-10. <https://doi.org/10.1111/j.1471-4141.2010.02222.x>
- Chang, K. C., Yoon, K., Robinson, A. E., & Koob, G. F. (2011). Methamphetamine and amphetamine induce neuroimmune activation in the nucleus accumbens. *Journal of Neurochemistry*, *116*(1), 1-10. <https://doi.org/10.1111/j.1471-4141.2010.02222.x>
- Chang, K. C., Yoon, K., Robinson, A. E., & Koob, G. F. (2011). Methamphetamine and amphetamine induce neuroimmune activation in the nucleus accumbens. *Journal of Neurochemistry*, *116*(1), 1-10. <https://doi.org/10.1111/j.1471-4141.2010.02222.x>
- Chang, K. C., Yoon, K., Robinson, A. E., & Koob, G. F. (2011). Methamphetamine and amphetamine induce neuroimmune activation in the nucleus accumbens. *Journal of Neurochemistry*, *116*(1), 1-10. <https://doi.org/10.1111/j.1471-4141.2010.02222.x>
- Chang, K. C., Yoon, K., Robinson, A. E., & Koob, G. F. (2011). Methamphetamine and amphetamine induce neuroimmune activation in the nucleus accumbens. *Journal of Neurochemistry*, *116*(1), 1-10. <https://doi.org/10.1111/j.1471-4141.2010.02222.x>
- Chang, K. C., Yoon, K., Robinson, A. E., & Koob, G. F. (2011). Methamphetamine and amphetamine induce neuroimmune activation in the nucleus accumbens. *Journal of Neurochemistry*, *116*(1), 1-10. <https://doi.org/10.1111/j.1471-4141.2010.02222.x>
- Chang, K. C., Yoon, K., Robinson, A. E., & Koob, G. F. (2011). Methamphetamine and amphetamine induce neuroimmune activation in the nucleus accumbens. *Journal of Neurochemistry*, *116*(1), 1-10. <https://doi.org/10.1111/j.1471-4141.2010.02222.x>

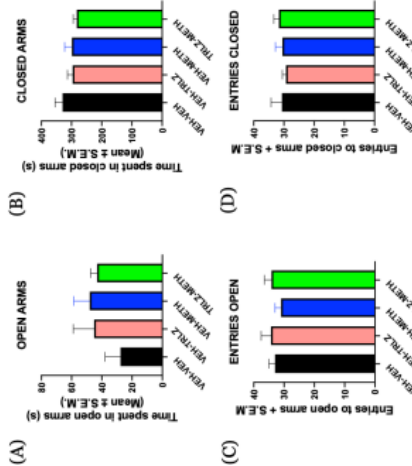


Figure 2 Chronic TRLZ did not have an anxiolytic effect on mice with chronic METH exposure in the elevated plus maze (EPM) (Fig. 2). (A) Time spent in open arms (s) (Mean ± S.E.M). (B) Time spent in closed arms (s) (Mean ± S.E.M). (C) Entries into open arms (Mean ± S.E.M). (D) Entries into closed arms (Mean ± S.E.M). Data were analyzed using one-way ANOVA.

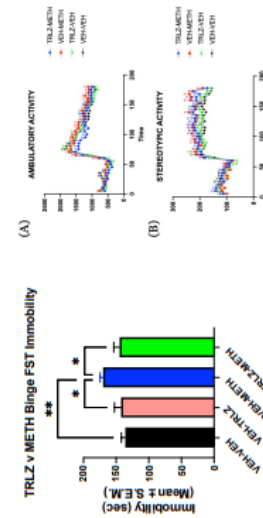


Figure 3 Chronic TRLZ did not have an anxiolytic effect on mice with chronic METH exposure in the elevated plus maze (EPM) (Fig. 2). (A) Ambulatory activity (Mean ± S.E.M). (B) Stereotypic activity (Mean ± S.E.M). Data were analyzed using one-way ANOVA.

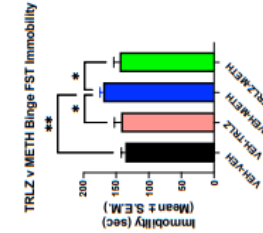


Figure 4 Chronic TRLZ increased immobility time in the FST in mice with chronic METH exposure. A one-way ANOVA revealed significant effects of METH and TRLZ (P < 0.0005). A Fisher's LSD multiple comparisons test with VEH as the control revealed significant differences between VEH and METH (P < 0.0005), VEH and TRLZ (P < 0.0005), and TRLZ and METH (P < 0.0005). Data presented as mean ± S.E.M.

This work was supported by NIDA grant R01DA051205 (SMR).

Acknowledgements



Investigating Y155 Phosphorylation of Protein Kinase C δ on Platelets as a Model for Neuronal Disease Mechanisms.

Dhruv N Vajipayajula*, Carol Dangelmaier, Monica Wright, and Satya P Kunapuli.

Lewis Katz School of Medicine

Sol Sherry Thrombosis Research Center, Lewis Katz School of Medicine at Temple University, Philadelphia, PA

Abstract

Neurons and platelets, although vastly different in origin and function, exhibit several similarities in their molecular composition and signaling mechanisms. This paper attempts to evaluate platelets as "circulating mirrors of neurons", with a particular focus on Protein Kinase C- δ (PKC δ). PKC δ is involved in many neuronal disease states including inflammation and degeneration. We demonstrate that PKC δ phosphorylation at the Y155 residue occurs specifically in response to the activation of the Glycoprotein receptor VI pathway (GPVI), physiologically stimulated by collagen. Using PKC δ Y155 knock-in mice, we show its involvement in GPVI mediated platelet activation and thrombus formation both ex-vivo and in-vivo. Our findings suggest a specific role for Y155 phosphorylation in PKC δ -associated signaling. We underscore the potential of platelets as accessible models for neuronal signaling pathways and we propose implications of PKC δ Y155 phosphorylation in probing neurodegenerative and inflammatory disease processes.

Background

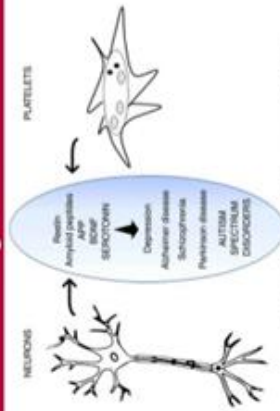


Figure 1. Similarities between Neurons and Platelets.

- There are many similarities between neurons and platelets (see Fig. 1). Platelets possess various intracellular granules, which bear a striking resemblance to presynaptic vesicles in neurons. They too store neurotransmitters such as serotonin, glutamate, dopamine, histamine, and ATP1. For exocytosis, both platelet degranulation and synaptic release engage the VAMP and SNARE mechanisms. Moreover, alterations of platelet function are often associated with neurological disorders and have been found to somehow mirror abnormalities observed in neurons¹. Thus, platelets are touted as "circulating mirrors of neurons."
- The focus of this project would be Protein Kinase C-delta (PKC δ), a serine/threonine kinase that is a critical regulator of the inflammatory response in the Central Nervous System (CNS). It has been shown in recent studies that PKC δ activation through GPVI, a collagen receptor, compromises the structural and functional integrity of the blood-brain barrier². It is also suggested that PKC δ is localized to intracellular neurofibrillary tangles of Tau protein in the Alzheimer's disease affected brain³.

- Of the several tyrosine residues on PKC δ , Y155 is selectively phosphorylated by GPVI agonists. Therefore, we generated PKC δ Y155F knock-in mice to investigate Y155 phosphorylation in platelets.

Methods

Human blood was collected from informed healthy donors and platelets were isolated by centrifugation in Tyrode's buffer. PKC δ Y155F and age matched littermate control (Wildtype) mice were bred, and blood was obtained through cardiac puncture. Platelets were isolated in Tyrode's buffer. On addition of agonists, platelet aggregation and ATP secretion were simultaneously detected using a lumi-aggregometer. Reactions were stopped with one-tenth volume of 6.6N perchloric acid to precipitate proteins, from which lysate samples were prepared for Western blotting. Human and murine platelet lysate were then subjected to SDS-PAGE (8% acrylamide) and were electro-transferred onto nitrocellulose membrane, incubated with antibodies, and imaged using an infrared scanner. To measure in-vivo thrombosis in mice, the Ferric chloride vascular injury model was used. Data was represented as mean \pm SE of at least three independent experiments and analyzed using student's t-test.

Results



Figure 2. Western blots of human platelet lysate on stimulation with Thrombin (100 U/mL) and convulxin (100 ng/mL). Y155 phosphorylation only occurs on GPVI activation.

- PKC δ Y155 is phosphorylated as early as 15 seconds in human platelets

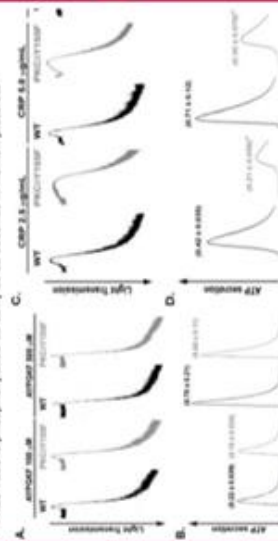


Figure 3. Representative aggregation (A & C) and dense granule secretion (B & D) of washed murine platelets from PKC δ Y155F knock-in mice and wild-type controls treated with varying concentrations of ADP/ATP (100 nM, 1 μ M, 10 μ M) and CRP (0.1 μ g/mL, 1 μ g/mL, 10 μ g/mL).

- This indicates that PKC δ Y155 positively regulates GPVI-mediated platelet activity

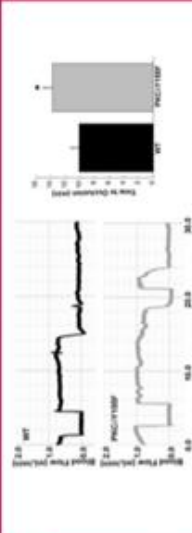


Figure 4. Ferric chloride vascular injury model. Time to vessel occlusion of murine carotid artery upon FCK3-injury is compared. PKC δ Y155F mice had longer time to occlusion compared to the WT littermate controls.

Discussion

- PKC δ Y155 phosphorylation occurs only downstream of GPVI pathways but not by GPCR pathways. PKC δ Y155F platelets exhibited diminished GPVI-mediated dense granule secretion specifically downstream of the GPVI pathway. Moreover, PKC δ Y155F mice exhibited diminished thrombus formation in-vivo.
- PKC δ in general negatively regulates GPVI-mediated dense granule secretion in platelets⁴. However, in this study, we provide evidence that PKC δ Y155 positively regulates dense granule secretion downstream of the GPVI pathway.
- One explanation could be that the PKC δ might bind to other signaling molecules, at sites other than Y155.
- There is another possibility that, upon Y155 phosphorylation, PKC δ is involved in regulating the function of Splice tyrosine kinase (SYK), a crucial signaling molecule involved in this cascade⁵.
- We can conclude that PKC δ Y155 phosphorylation is specific to the GPVI pathway in human platelets, and it positively regulates GPVI-mediated platelet activity.
- We have proven that blood platelets serve as an effective and accessible model for simulating signaling pathways in neurons. This raises the possibility of PKC δ Y155 phosphorylation having a distinct role to play in neurodegenerative and inflammatory mechanisms in the nervous system. For further investigation, it is recommended to verify the signaling in neuronal cells through selective transfection of a PKC δ Y155 knock-in gene.

References

- Caraballo, G.A., Soria, M. (2017). Platelets in Neurological Disorders. In: Grimaldi, R., Klemm, M., Lopez, J., Page, C. (eds) Platelets in Thrombotic and Neurothrombotic Disorders. Springer, Cham.
- Espartero, J. and Espartero, J.D. (2012) The Role of Platelets in the Modulation of Neuronal Synaptic Plasticity. Front. Cell. Neurosci. 6:100. doi:10.3389/fncel.2012.00100
- Tang, T., Samson, J., Sun, S., et al. Protein kinase C-delta inhibition protects blood-brain barrier from sepsis-induced vascular damage. J Neuroinflammation 13, 100 (2016).
- Wang, Y., Wang, Y., Wang, Y., et al. Platelet-derived serotonin regulates platelet functional responses. J Biol Chem 286(12):10111-10116 (2011).
- D. & Naranjo, C.L. (2015). Current mechanisms of Alzheimer's disease and ischemic stroke: the role of protein kinase C in the progression of age-related neurodegeneration. Journal of Alzheimer's disease: JAD, 48(1), 711-724.
- Chen, Y., Wang, Y., Wang, Y., et al. Platelet-derived serotonin regulates platelet functional responses. J Biol Chem 286(12):10111-10116 (2011).
- Probst, A., Dillies, J.M., Jurek, M., van Vlymen, I.G., Saks, T., Tyhonen, V.L., & Watanabe, S. (1997). The K+ receptor gamma-chain and the tyrosine kinase Syk are essential for activation of mouse platelets by collagen. The EMBO journal, 16(16), 4119-4124.

Acknowledgements

- Temple University College of Science and Technology
- Sol Sherry Thrombosis Research Center
- Dr. Satya P Kunapuli, Carol Dangelmaier, and Monica Wright

SEMINAR

Speaker: Dr. Vincenzo Carnevale

Bruce Taggart Associate Professor

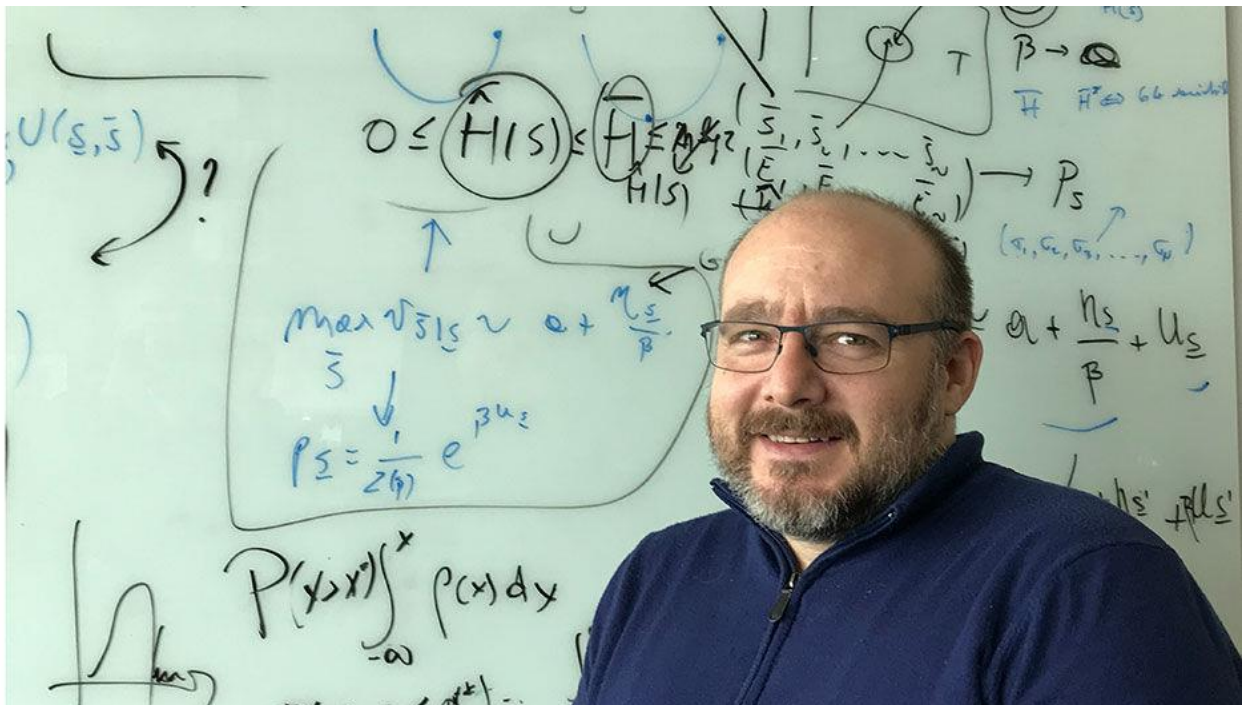
Department of Biology

Institute for Computational Molecular Science (ICMS)

Institute for Genomics and Evolutionary Medicine (IGEM)

Temple University

Philadelphia, PA



Host: Dr. Eleni Anni – eleni.anni@temple.edu

From Genetic Blueprints to Biological Function: Unraveling the Complexity of Ion Channels

Abstract

Ion channels, nature's intricate nanodevices, play a crucial role in controlling transmembrane potential and propagating electrical signals. Through natural selection, a diverse array of ion channels has evolved, each uniquely responsive to specific environmental stimuli. From a thermodynamic perspective, transitions between their operational states - such as opening or closing - are influenced by generalized forces including temperature, external electric fields, and surface tension. Remarkably, certain ion channels are polymodal, capable of activation through multiple distinct stimuli. Among these, transient receptor potential channels (TRP channels) are particularly versatile, responding to extreme temperatures, various ligands, pH levels, and hydrostatic pressure to relay sensory information across numerous organisms. In my research group, we delve into the molecular underpinnings of ion channel functionality. During this talk, I will showcase our latest findings from molecular simulations and machine learning analyses. Our studies reveal that specific clusters of co-evolved amino acids endow channels with their temperature sensitivity or voltage-driven gating capabilities. Further, I will explore how these molecular insights have enabled us to perform targeted in silico drug screening, enhancing our understanding of the structural determinants critical for ion channel function and their pharmacological inhibition.

DISTINCTION IN MAJOR



BIOLOGY

MOLLY KENNELLY

VIOLET LANGE

LOGAN MCCULLOUGH

ROHAN HAROLIKAR

IMENE MANCER

KELLY MEINERT

SRAAVYA PINJALA

VRUNDA SATASIYA

FAIZ H SIDDIQUI

CELLULAR & MOLECULAR NEUROSCIENCE

SAMHITHA BALAJI

BHARGAV BULUSU

NIKKI DIETZ

TAYLOR FORRY

ESTHER EDET IKPEME

GANESH MURUGANANDAM

OLA SZMACINSKI

DHRUV VAJIPAYAJULA

MADISON WOLF

KURALAI ZHOLDOSH KYZY

FULBRIGHT GRADUATE DEGREE GRANT



SAMHITHA BALAJI

CELLULAR & MOLECULAR NEUROSCIENCE

Samhitha, a senior student in the Department of Biology, will do research in Translational Neuroscience as part of the MS program at the University of Sheffield, U.K. She embodies the “rigor in scholarly enquiry and academic excellence” and “flexibility and dynamism” that the award is looking for in its applicants.

RESEARCH ADVISORS

Thank you to all the mentors for their training and support of
the students

DR. KARIM BAHMED

DR. MARIANA BONFIM

DR. PARKSON LEE-GAU CHONG

DR. STEPHANIE DAWS

DR. NORA ENGEL

DR. SILVIA FOSSATI

DR. ERICA GOLEMIS

DR. DIA HALALMEH

DR. MATTHEW R. HELMUS

DR. SHIN KANG

DR. JOHN KARANICOLAS

DR. BARBARA KRYNSKA

DR. SUDHIR KUMAR

DR. SATYA P KUNAPULI

DR. HAYAN LEE

DR. SHUXIN LI

DR. DAVID LIBERLES

DR. SADIA MOHSIN

DR. ANDREA MORRIONE

DR. MARIA PACHECO

DR. SERGEI POND

DR. GILLIAN QUEISSER

DR. SCOTT RAWLS

DR. ILKER K. SARIYER

DR. BRENT SEWALL

DR. GEORGE SMITH

DR. GREGORY SMUTZER

DR. JONATHAN SOBOLOFF

DR. RACHEL SPIGLER

DR. ELLEN UNTERWALD

DR. SARA JANE WARD

DR. JINHUA WU

RETIREMENT
celebration



Come join us in honoring

Evelyn Vleck

MONDAY, APRIL 29, 2024

At 3:30 with a reception to follow

Gladfelter 21 & SERC Lobby

ACKNOWLEDGMENTS

Thank you to everyone who made this Research Day possible

Faculty Advisors

Dr. Eleni Anni, Cellular and Molecular Neuroscience, Organizer

Dr. Caryn Babaian, Genomic Medicine

Dr. Angela Bricker, Biology

Dr. Brent Sewall, Ecology, Evolution and Biodiversity

Dr. Evelyn Vleck, Transfer students, Co-organizer

Research Liaisons

Dr. Jay Lunden

Dr. Jody Hey

Dr. Frank Nelson

Administrative Support

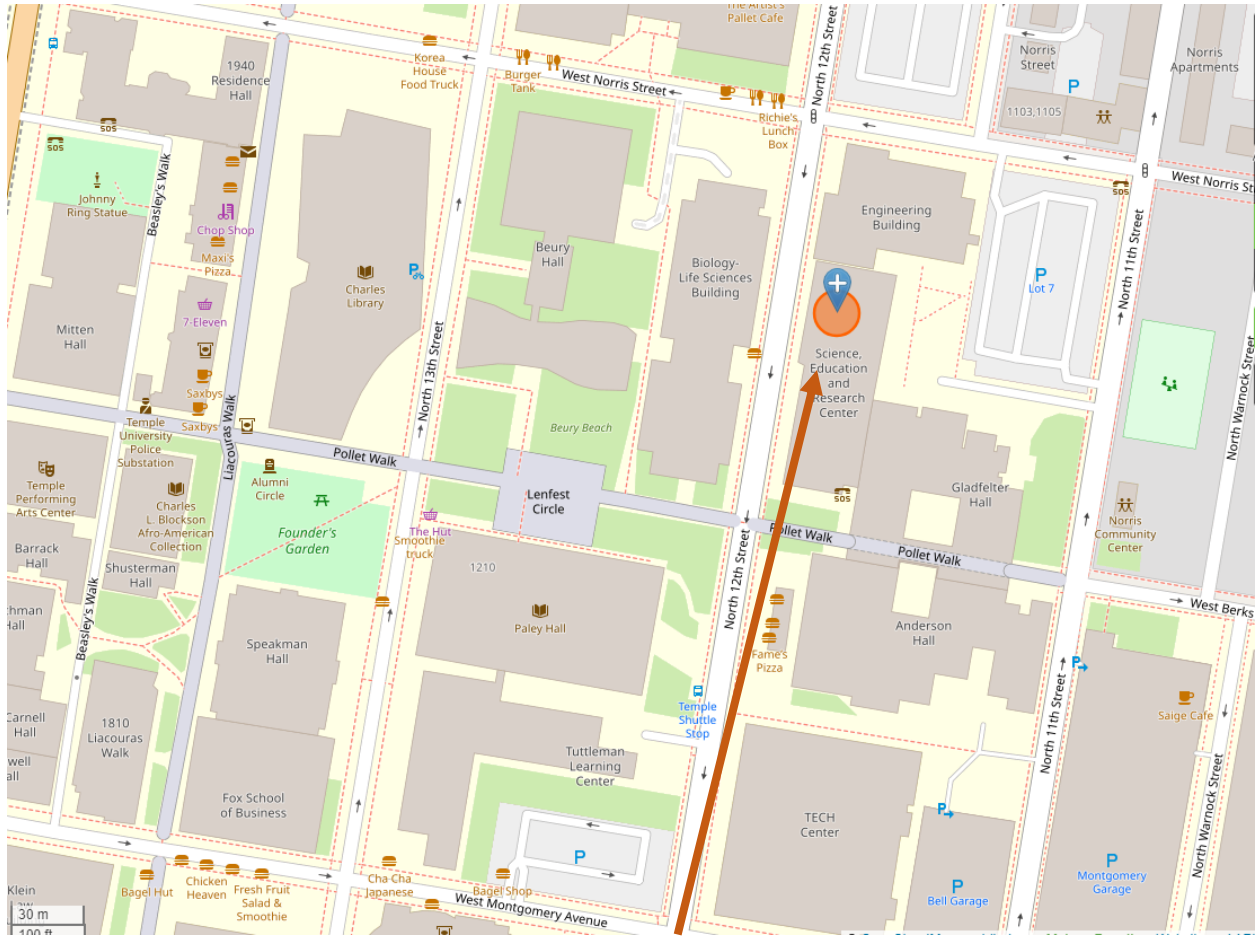
Chivonne Matthews, Sr Department Administrative Specialist

Toni Matthews, Senior Business Manager

Administration

Dr. Robert Sanders, Chair

Dr. Erik Cordes, Vice Chair



SERC and Gladfelter Buildings

For additional information contact Eleni.Anni@temple.edu